

ANALYSIS OF DATA FROM THE BARNETT SHALE WITH CONVENTIONAL
STATISTICAL AND VIRTUAL INTELLIGENCE TECHNIQUES

A Thesis

by

OBADARE OLUSEGUN AWOLEKE

Submitted to the Office of Graduate Studies of
Texas A&M University
in partial fulfillment of the requirements for the degree of

MASTER OF SCIENCE

December 2009

Major Subject: Petroleum Engineering

ANALYSIS OF DATA FROM THE BARNETT SHALE WITH CONVENTIONAL
STATISTICAL AND VIRTUAL INTELLIGENCE TECHNIQUES

A Thesis

by

OBADARE OLUSEGUN AWOLEKE

Submitted to the Office of Graduate Studies of
Texas A&M University
in partial fulfillment of the requirements for the degree of

MASTER OF SCIENCE

Approved by:

Chair of Committee,	Robert Lane
Committee Members,	Gioia Falcone
	Yoonsuck Choe
Head of Department,	Stephen A. Holditch

December 2009

Major Subject: Petroleum Engineering

ABSTRACT

Analysis of Data from the Barnett Shale with Conventional Statistical and Virtual Intelligence Techniques. (December 2009)

Obadare Olusegun Awoleke, B.Sc., University of Ibadan, Nigeria

Chair of Advisory Committee: Dr. Robert Lane

Water production is a challenge in production operations because it is generally costly to produce, treat, and it can hamper hydrocarbon production. This is especially true for gas wells in unconventional reservoirs like shale because the relatively low gas rates increase the economic impact of water handling costs. Therefore, we have considered the following questions regarding water production from shale gas wells: (1) What is the effect of water production on gas production? (2) What are the different water producing mechanisms? and (3) What is the water production potential of a new well in a given gas shale province.

The first question was answered by reviewing relevant literature, highlighting observed deficiencies in previous approaches, and making recommendations for future work. The second question was answered using a spreadsheet based Water-Gas-Ratio analysis tool while the third question was investigated by using artificial neural networks (ANN) to decipher the relationship between completion, fracturing, and water production data. We will consequently use the defined relationship to predict the average water production for a new well drilled in the Barnett Shale. This study also derived

additional insight into the production trends in the Barnett shale using standard statistical methods.

The following conclusions were reached at the end of the study:

- 1) The observation that water production does not have long term deleterious effect on gas production from fractured wells in tight gas sands cannot be directly extended to fractured wells in gas shales because the two reservoir types do not have analogous production mechanisms.
- 2) Based on average operating conditions of well in the Barnett Shale, liquid loading was found to be an important phenomenon; especially for vertical wells.
- 3) A neural network was successfully used to predict average water production potential from a well drilled in the Barnett shale. Similar methodology can be used to predict average gas production potential.

Results from this work can be utilized to mitigate risk of water problems in new Barnett Shale wells and predict water issues in other shale plays. Engineers will be provided a tool to predict potential for water production in new wells.

DEDICATION

This thesis is dedicated to God, who is the Custodian of all knowledge. And To my parents, without whom, I would not have been.

It is also dedicated to my sister, Enitan, and her son, Derin.

ACKNOWLEDGEMENTS

I thank my committee chair, Dr. Lane, for taking me on as his student and for his advice and understanding on both technical and personal issues throughout the duration of my degree.

I thank Dr. Falcone for agreeing to be a member of my committee and for clarifying issues related to liquid loading in gas wells.

I also thank Dr. Choe for agreeing to be a member of my committee and for patiently explaining the fundamentals of neural networks to me both; in class and in conversations at his office.

Thanks also go to my friends and colleagues, and the departmental faculty and staff, for helping me to adjust to this environment. I also want to extend my gratitude to the Crisman Institute of the Petroleum Engineering Department for funding part of this work.

Finally, thanks to my family for their support, understanding and love.

TABLE OF CONTENTS

	Page
ABSTRACT	iii
DEDICATION	v
ACKNOWLEDGEMENTS	vi
TABLE OF CONTENTS	vii
LIST OF FIGURES.....	ix
LIST OF TABLES	xiv
1. INTRODUCTION.....	1
1.1 Statement of Problem	1
1.2 Background and Literature Review.....	2
1.2.1 Literature review on the effect of water production on gas production in shale gas reservoirs	2
1.2.2 Literature review on the determination of water production mechanisms in unconventional gas reservoirs	5
1.2.3 Literature review on the use of artificial neural networks in petroleum engineering.....	6
1.3 Objectives of Research.....	9
1.4 Outline of Thesis	9
2. ANALYSIS OF PRODUCTION DATA IN THE BARNETT SHALE.....	11
2.1 Geological Overview of the Barnett Shale.....	11
2.2 General Analysis of Data from the Barnett Shale	14
2.3 Effect of Water Production on Gas Well Productivity	27
2.4 Section Summary	29
3. ANALYSIS OF WATER PRODUCTION MECHANISMS IN THE BARNETT SHALE	31
3.1 Water-Hydrocarbon Ratio and Water-Hydrocarbon Ratio Derivative Analysis in Conventional Reservoirs	31

	Page
3.2 Water-Hydrocarbon Ratio and Water-Hydrocarbon Ratio Derivative Analysis in Unconventional Reservoirs	33
3.3 Load Water Recovery Factor in Denton and Parker Counties of the Barnett Shale	37
3.4 Section Summary	40
4. PRODUCTION DATA ANALYSIS USING NEURAL NETWORKS.....	41
4.1 Introduction	41
4.2 Machine Learning Concepts.....	42
4.3 Neural Network Theory	46
4.4 Determination of Training Set Size.....	54
4.5 Determination of Hidden Structure in Data	57
4.6 Determination of Whether a Well Drilled in Denton County of the Barnett Shale Will Produce Water	68
4.7 Prediction of Average Water Production for A New Well Drilled in the Denton and Parker Counties of the Barnett Shale.....	73
4.8 Prediction of Well Rank Using Parameters Contained in Neural Network Input Vector.....	80
4.9 Section Summary	83
5. CONCLUSIONS AND RECOMMENDATIONS.....	84
5.1 Conclusions	84
5.2 Recommendations	85
REFERENCES.....	86
APPENDIX A	99
VITA	102

LIST OF FIGURES

FIGURE	Page
2.1 Generalized Stratigraphic Column, Fort Worth Basin. Expanded section shows more detailed interpretation of Mississippian stratigraphy. V-S refers to Viola Simpson interval (from Montgomery et al., 2005)	12
2.2 (A) Area determined where Viola Limestone or Simpson Group is present. Dotted rectangle represents area shown in (B). (B) Map showing subcrop geology of the Barnett Shale (modified from Pollastro et al., 2005)	13
2.3 Percentage breakdown of wells in the Barnett Shale based on well type (data from HPDI)	16
2.4 Relationship between cumulative gas and water production in conventional reservoirs of the Fort Worth basin.....	17
2.5 Relationship between cumulative gas and water production in unconventional reservoirs of the Fort Worth basin	17
2.6 Relationship between cumulative gas and water production in core area of the Barnett Shale	18
2.7 Relationship between cumulative gas and water production in non-core area of the Barnett Shale	18
2.8A P50 values for gas production (deviated wells).....	20
2.8B P50 values for gas production (horizontal wells)	20
2.8C P50 values for gas production (vertical wells)	21
2.9A P50 values for water production (deviated wells)	21
2.9B P50 values for water production (horizontal wells).....	22
2.9C P50 values for water production (vertical wells).....	22
2.10 Number of wells completed in Denton County by type per year	24
2.11 Number of wells completed in Parker County by type per year	24

FIGURE	Page
2.12 P50 values for average gas production every year in Denton County (horizontal wells).....	25
2.13 P50 values for average gas production every year in Parker County (horizontal wells).....	25
2.14 P50 values for average water production every year in Denton County (horizontal wells).....	26
2.15 P50 values for average water production every year in Parker County (horizontal wells).....	26
2.16 Predictive chart for onset of liquid loading in the Barnett Shale	29
3.1A Water coning and channeling WOR comparison plot.....	31
3.1B Multi-layer channeling WOR and WOR derivative plot.....	32
3.1C Bottom water coning WOR and WOR derivative plot.....	32
3.2A WGR plots in Barnett Shale (Type 1)	34
3.2B WGR plots in Barnett Shale (Type 2)	35
3.2C WGR plots in Barnett Shale (Type 3)	36
3.2D WGR plots in Barnett Shale (Type 4)	36
3.3 Liquid loading mechanisms description.....	37
3.4A CDF plot of Load Recovery Factor (LRF) for deviated wells in Denton County	38
3.4B CDF plot of Load Recovery Factor (LRF) for horizontal wells in Denton County	38
3.4C CDF plot of Load Recovery Factor (LRF) for vertical wells in Denton County	39
3.5A CDF plot of Load Recovery Factor (LRF) for horizontal wells in Parker County	39

FIGURE	Page
3.5B CDF plot of Load Recovery Factor (LRF) for vertical wells in Parker County	40
4.1 Neural network as a function approximator, f , between input and output parameters	44
4.2 Representation of non-linear model of a neuron (modified from Haykin, 2005).....	49
4.3A Log-sigmoid function plot (Haykin, 2005)	50
4.3B Hyperbolic tangent function plot (Haykin, 2005)	51
4.4A Representation of a single layer feed-forward network (Haykin, 2005)....	52
4.4B Representation of a multi layer feed-forward network (Haykin, 2005)	52
4.4C Representation of a recurrent neural network (Haykin, 2005)	53
4.5 Block diagram of a neural network, highlighting the only neuron in the output layer (Haykin, 2005)	53
4.6 Dependence of training set size on error bounds	56
4.7 Two-dimensional distribution produced by a linear input-output mapping (Haykin, 2005)	58
4.8 Kohonen model of a self-organized map (modified from Haykin, 2005)..	60
4.9 2D SOM topology using 10x10 neurons with rectangular grid blocks topology.....	62
4.10 Color-coded representation of self organized map neighbor weight distances for deviated, horizontal and vertical wells, number of iterations =100.....	63
4.11 2D SOM layer for all wells with each neuron showing the number of input vectors that it classifies, number of iterations = 100, number of examples = 450.....	64
4.12 Color-coded representation of self organized map neighbor weight distances for 20 high water producers, number of iterations=100	64

FIGURE	Page
4.13 2D SOM layer for all wells with high water production with each neuron showing the number of input vectors that it classifies, number of iterations = 100, number of examples = 20.....	65
4.14 Silhouette plot for dataset.....	67
4.15 Output and input of feed-forward neural network for water production potential classification.....	69
4.16 Results of feed-forward neural network for classification purposes.....	70
4.17 Block diagram of adaptive pattern classification, using a SOM and a learning vector quantizer (Haykin, 2005)	71
4.18 Influence of ‘rank’ on neural network performance; performance on training, testing and validation datasets (rank in input vector, target is logarithm of water production)	74
4.19 Neural network performance, rank not in input vector (target is logarithm of water production)	75
4.20 Neural network performance (rank in input vector, target is ‘raw’ water production)	75
4.21 Network output versus target for vertical wells in Parker County, rank included. Dataset size =58 (number of hidden layers =1; number of neurons in hidden layer =8).....	78
4.22 Network output versus target for horizontal wells in Parker County, rank included. Dataset size =219 (number of hidden layers =1; number of neurons in hidden layer =5).....	78
4.23 Network output versus target for vertical wells in Denton County, rank included. Dataset size =250 (number of hidden layers =1; number of neurons in hidden layer =10).....	79
4.24 Network output versus target for horizontal wells in Denton County, rank included. Dataset size =219 (number of hidden layers =1; number of neurons in hidden layer =5).....	79
4.25 Dot product of normalized input vectors in training dataset.....	81

FIGURE	Page
4.26 P10, P50 and P90 predictions of water production for horizontal wells drilled in the Parker County of the Barnett Shale	82
4.27 P10, P50 and P90 predictions of gas production for horizontal wells drilled in the Parker County of the Barnett Shale	82

LIST OF TABLES

TABLE	Page
1.1 Application of artificial neural networks in petroleum engineering literature	7
2.1 Distribution of wells in the non-core and core counties of the Barnett Shale as at December 31st, 2008.....	15
2.2A Statistical analysis of data from Denton County	23
2.2B Statistical analysis of data from Parker County	23
2.3 Parameters used to investigate liquid loading in the Barnett Shale	27
4.1 Neural network component summary	56
4.2 Parameters in input vector for Denton and Parker Counties	61
4.3 Average silhouette values for increasing number of clusters.....	67
4.4 Summary of results for competitive neural network	71
4.5 Summary of results for vector quantizer	72
4.6 Influence of rank on network performance	76
4.7 Summary of neural network result runs	77

1. INTRODUCTION

1.1 Statement of Problem

Some work has been done on the effect of hydraulic fracture load water production on gas production in tight gas reservoirs. However, in all these publications, the potential effects water from other sources was not considered. Work has also been done on characterizing water production mechanisms in conventional hydrocarbon reservoirs on the basis of the analysis of Water-Oil-ratio (WOR) and Water-Gas-Ratio (WGR) data over time. This technique has not been applied to understanding the water production mechanisms in unconventional gas reservoirs. We have also noted that large bodies of data relating to fracturing operations in gas shales exist in public databases. These databases also contain production data. In this work, firstly, we examine production figures from the Barnett Shale using conventional statistical techniques. Secondly, we also extend Chan's work (1995) on water control diagnostic plots to unconventional gas reservoirs. Lastly, it is pertinent to note that few attempts has been made to investigate the relationship between water production from shale gas reservoirs and well / reservoir and fracturing treatment data. This is not surprising because this relationship is very complex. Therefore, we attempt to use neural networks to decipher the relationship between water production and parameters related to the well, completion, reservoir and the hydraulic fracture. This method was chosen because of the proven ability of neural networks to model complex relationships between variables.

This thesis follows the style of *SPE Journal*.

1.2 Background and Literature Review

We will be tackling a broad spectrum of issues in this research work. It is only expedient that an independent literature review be conducted for each facet of our investigation. Therefore, this section of the thesis is sub-divided into three parts:

- (a) Literature review on the effect of water production on gas production in shale gas reservoirs.
- (b) Literature review on the determination on water production mechanisms in unconventional gas reservoirs.
- (c) Literature review on the application of artificial neural networks in petroleum engineering.

1.2.1 Literature review on the effect of water production on gas production in shale gas reservoirs

There is a paucity of papers in technical literature of the effect of water production on shale gas production. In order to have some understanding of this issue, we surveyed literature on the effect of water production in tight gas sands. These two reservoir types are not analogous, but a study of one might give us some insight into the behavior of the other.

Tannich (1975) investigated the process of liquid removal from hydraulically fractured gas wells using a numerical model. He modeled four physical processes that were coupled to illustrate the clean-up problem. The processes include: (1) two-phase 1-D flow of fluid in the tubing, (2) fluid behavior in the fracture, (3) flow in the liquid invaded region, neglecting capillary and gravitational forces, and (4) single phase flow of gas in the un-invaded portions of the reservoir. Regarding this issue, he concluded that:

(1) clean-up efficiency is greatest when the fracture is short and highly conductive (2) permanent productivity damage is not likely if the fracture conductivity is high relative to the formation permeability.

Holditch (1979) evaluated the factors affecting water and gas flow from hydraulically fractured gas wells. He concluded that the most important criteria include the mobility of water in the reservoir, the total pressure drawdown, extent/depth of formation damage and the magnitude of the capillary discontinuity between the fracture and the reservoir. The short and long term behavior of gas wells in tight gas reservoirs is governed primarily by these factors. The main difference between Holditch and Tannich's work is that Holditch includes the effect of capillary pressure in the invaded zone in his model. The effect of a water block is negligible if the pressure drawdown is large compared to the capillary pressure end effects in the formation or if the water mobility is high. This ensures the fluid bank is easily imbibed into the reservoir enabling optimum gas production. The converse is the case if the pressure drawdown and the capillary pressure in the reservoir are comparable. The effect of capillary pressure in the invaded zone is exacerbated by the presence of skin.

Soliman et al. (1985) contributed to this discourse by using a reservoir simulator to emphasize the importance of fracture conductivity to the clean up process. They concluded that at low conductivities, the gas breakthrough into the fracture occurs near the wellbore. This phenomenon impacts negatively on clean-up efficiency. As fracture conductivity increases, the saturation distribution around the fracture in the invaded zone becomes more uniform with a resulting increase in clean-up efficiency. They noted that for a hydraulic fracture, there exists an optimum dimensionless conductivity for the back-

production of fracturing fluid. This optimum conductivity is usually more than what is required for peak gas production. They also concluded that in some cases, the clean up of fracturing fluids might largely be controlled by the magnitude of difference between the capillary pressure and the drawdown. Soliman et al. focused on the short term effect of these parameters on gas production and water recovery.

Iqbal (1998) developed a multi-phase and multi-dimensional simulator to evaluate the liquid cleanup performance of hydraulically fractured wells with consideration of skin effect caused by clay swelling and migration of fines. He agreed with Holditch's conclusions as stated above.

Montgomery et al. (1990) simulated the fluid invasion by injecting water in an open high conductivity fracture. The hydraulic fracture treatment is simulated in three stages, namely: (1) an injection period to simulate fracturing leak-off and imbibition into the formation, (2) a shut-in period to simulate fracture pressure bleed-off and fracture closure, (3) a production period to simulate flow back of fracturing fluids and gas production. According to them, the parameters that determine whether poor fracturing fluid recovery reduces the productivity of hydraulically fractured wells are: (1) fracture conductivity (2) formation damage to fracture face (3) relative permeability hysteresis in the invaded zone.

Friedel et al. (2007) took a panoramic view of the clean up process in fractured gas wells. They characterized the causes of sub-optimal production to two broad subdivisions – (a) those artificially induced as a result of the fracturing process and (b) natural process independent of fracturing like stress related permeability reduction. The artificial causes included productivity impairment due to the presence of a load water

invasion zone. The focus of their work was to investigate the effect of all these factors using a single simulator because of the interdependence of the causes of sub-optimal production. One of their conclusions is that hydraulic damage due to the load water does not impair productivity on the long term. The reservoir pressure used for their simulations is however very high (9000 psi). They did not consider a low – pressure case. Possible mechanisms of impairment include but are not limited to; (1) 3-phase flow (2) formation of a load-water invasion zone accompanied by hydraulic and mechanical damage in the fracture vicinity (3) filter cake build up and erosion (4) proppant pack conductivity reduction due to gel residue (5) unbroken fracturing fluids in the proppant pack (f) inertial or non-Darcy flow (6) geo-mechanical effects.

1.2.2 Literature review on the determination of water production mechanisms in unconventional gas reservoirs

There is a paucity of work on the different mechanisms of water production in unconventional gas reservoirs. In the same vein, the body of literature on determining the mechanism of water production using production data is virtually non-existent. The paucity of information in this area of petroleum engineering may be due to the highly non-unique nature of most proposed solutions. The possible mechanisms of water production in conventional reservoirs were investigated by Seright et al. (2003). For characterizing water production mechanism using production data in conventional reservoirs, Chan (1995) in his seminal paper on the subject matter classified these mechanisms based on the shapes of the WOR and WOR' curves. Seright (1997) emphasized that Chan's methodology should not be used in isolation. The shape of the WOR and WOR derivative curves are dependent on the degree of vertical communication

and permeability contrast among layers, saturation distribution, pressure gradient in the reservoir, relative permeability / capillary pressure curves and vertical to horizontal permeability ratio. He concludes no particular trend is unique to either the coning or channeling problem. His conclusions do not vitiate Chan's work; it only implies the diagnostic plots developed by Chan should be used with caution.

1.2.3 Literature review on the use of artificial neural networks in petroleum engineering

Virtual Intelligence techniques in general and Artificial Neural Networks (ANN) in particular have been used to solve problems in the various branches of petroleum engineering. Shelley et al. (2008) used a self – organizing map to analyze the reservoir and stimulation data of Barnett shale wells fractured with either slick-water or cross-linked gels. They also attempted to develop a predictive model for well productivity by training a neural net. This attempt was unsuccessful. They speculated that this failure was caused by a lack of information necessary to fully describe reservoir quality or stimulation effectiveness. A detailed summary of the applications of artificial intelligence in petroleum engineering from SPE literature is shown in **Table 1.1**.

Table 1.1- APPLICATION OF ARTIFICIAL NEURAL NETWORKS IN PETROLEUM ENGINEERING LITERATURE

Summary Papers	Mohaghegh (2000a, 2000b, 2000c)
General Reservoir Engineering <ul style="list-style-type: none"> • Prediction of equilibrium 'k' values for light hydrocarbon mixtures; prediction of 2 or 3-phase relative permeabilities. 	Habiballah et al. (1996); Silpngarmlers (2002).
Well Test Interpretation <ul style="list-style-type: none"> • Well test interpretation modeling. 	Al-Kaabi et al. (1993), Athichanagorn et al. (1995), Kumoluyi et al. (1994, 1995).
Geostatistics, Reservoir Simulation and Data Integration. <ul style="list-style-type: none"> • Optimization of well placement. • Data Integration. • Geostatistics. • Neuro-simulation. • Upscaling 	Guyaguler et al.(2000), Yeten et al. (2002). Srinivasan et al. (2000), Arpat et al. (2001). Caers et al. (1998, 1999) Doraisamy (1998a), Doraisamy et al. (1998b), Centilmen et al.(1999), Chang et al. (2000), Ayala et al. (2005), Ayala et al. (2007), Gorucu et al. (2005), Ramgulam et al. (2007), Srinivasan et al. (2008), Artun et al. (2008), Demiryurek et al. (2008). Chawanthe et al. (1997).

Table 1.1 - CONTINUED	
Formation Evaluation and Reservoir Characterization.	
<ul style="list-style-type: none"> • Prediction of permeability, porosity and deep resistivity from well logs. 	Chawanthe et al. (1994); Mohaghegh et al. (1995a, 1995b, 1997); Wo et al. (2000); Basbug et al. (2007)
<ul style="list-style-type: none"> • Generation of synthetic Magnetic Resonance Imaging (MRI) logs from conventional well logs. 	Mohaghegh et al. (1998a, 2000e).
<ul style="list-style-type: none"> • Application of ANN in Reservoir Characterization. 	Aminian et al. (2002, 2003a, 2003b)
<ul style="list-style-type: none"> • Development of Surrogate Reservoir Models for analysis of complex reservoirs. 	Mohaghegh et al. (2006a); Mohaghegh (2006b)
<ul style="list-style-type: none"> • Permeability prediction in carbonate reservoirs. 	Lee Sang Heon et al. (2002)
<ul style="list-style-type: none"> • Fractured Reservoir Characterization; correlation of seismic attributes to reservoir properties. 	Ouenes et al. (1994, 1995); Zellou et al. (1995); Balch et al. (1999); Kaviani et al. (2008).
Water-flooding	
<ul style="list-style-type: none"> • Optimizing water flood performance 	Garg et al. (1996); Aminian et al. (2000)
Drilling	
<ul style="list-style-type: none"> • Prediction of Rate of Penetration (ROP) values. 	Bilgesu et al. (1997, 2000); Balch et al. (2002).
Hydraulic Fracturing	
<ul style="list-style-type: none"> • Hydraulic Fracture Treatment design 	Mohaghegh et al. (1996a, 1996b).
<ul style="list-style-type: none"> • Selection of stimulation / re-stimulation candidates 	Mohaghegh et al. (1998b, 1999, 2000d); Reeves et al. (1999a, 1999b)
Production	
<ul style="list-style-type: none"> • Pumping Unit Optimization; prediction of liquid hold up; identification of work-over candidates; water shut off candidate selection. 	Hosn et al. (2001), Mohaghegh et al. (2002); Shippen et al. ; (2004); Popa et al. (2005); Saeedi et al. (2007).
Production Forecasting	
<ul style="list-style-type: none"> • Forecasting natural gas production 	Al-Fattah et al. (2003), Garcia et al. (2004)

Table 1.1 - CONTINUED	
Data Mining	
<ul style="list-style-type: none"> • Identification of contaminated data in a dataset; identification of production drivers. 	Popa et al. (2003), Mohaghegh (2003), Wei et al. (2004); Shelley et al. (2009).
Data Analysis in the Barnett Shale	Shelley et al. (2008)

1.3 Objectives of Research

The objectives of this research work are as follows:

- Analyze gas and water production data from the Barnett Shale using simple statistical relations.
- Use the methodology developed by Chan (1995) to study water production data from the Barnett Shale to attempt to identify water production mechanism.
- Use Artificial Neural Networks (ANN) to investigate the relationship between water production and various fracturing and well parameters. This is necessary in order to be able to predict water production for a new well.

1.4 Outline of Thesis

As opposed to conventional thesis outlines that show a progression of work from model development to the presentation of results, this work will focus on different themes in each section.

In Section 2, we analyzed production and fracturing data from the Barnett Shale. As a matter of interest, we calculated the flow rate versus the minimum gas rate profile

required for the prevention of liquid loading in the Barnett Shale. We also summarized conclusions from previous work on the effect of water production on gas production.

In Section 3, we applied Chan's methodology for water influx mechanism determination to production data from the Barnett Shale. We identified some interesting trends and we proposed reasonable explanations for these trends. However, the development of a general conceptual framework to interpret these trends is recommended to be the focus of some future work.

In Section 4, we developed a neural network based tool that can be used to predict water production from a new well completed in the Barnett Shale.

In Section 5, we detail our conclusions from this study and recommendations for future work.

2 ANALYSIS OF PRODUCTION DATA IN THE BARNETT SHALE

2.1 Geological Overview of the Barnett Shale

The Fort Worth basin is an elongated wedge shaped basin in North Central Texas. At present, the Barnett Shale is one of the most sought after plays in the Fort Worth Basin. As shown in **Fig. 2.1**, the Barnett Shale is not the only exploration target in the Fort Worth basin. However, it is the only shale gas play. Detailed consideration of the geologic history of the Barnett Shale is presented by Pollastro et al. (2007). Nevertheless, we want to note the following:

1. Based mainly on stratigraphy, thermal maturity and Total Organic Carbon (TOC), the Barnett Shale is divided into the Core Area and the Non-Core Area (Pollastro et al. 2007). See **Fig. 2.2**.
2. All the wells are hydraulically fractured; most commonly with large volumes of proppant laden slick-water, (Martineau 2007).
3. In some areas, the Barnett Shale is enclosed in between dense and impermeable limestone (Core Area), while in some areas, one or both of the limestone barriers are absent (Non-Core Area). These limestone layers act as barriers to excessive hydraulic fracture height development. The limestone layer above the Barnett Shale is called the Forestburg limestone, while the one below the shale is called the Viola Limestone.
4. In the Fort Worth basin, a water bearing layer exists below the Barnett Shale. This layer can either lie directly below the Barnett Shale (Non-Core Area) or a

limestone barrier separates the shale and the water bearing layer (Core Area).

The water bearing layer is called the Ellenburger formation.

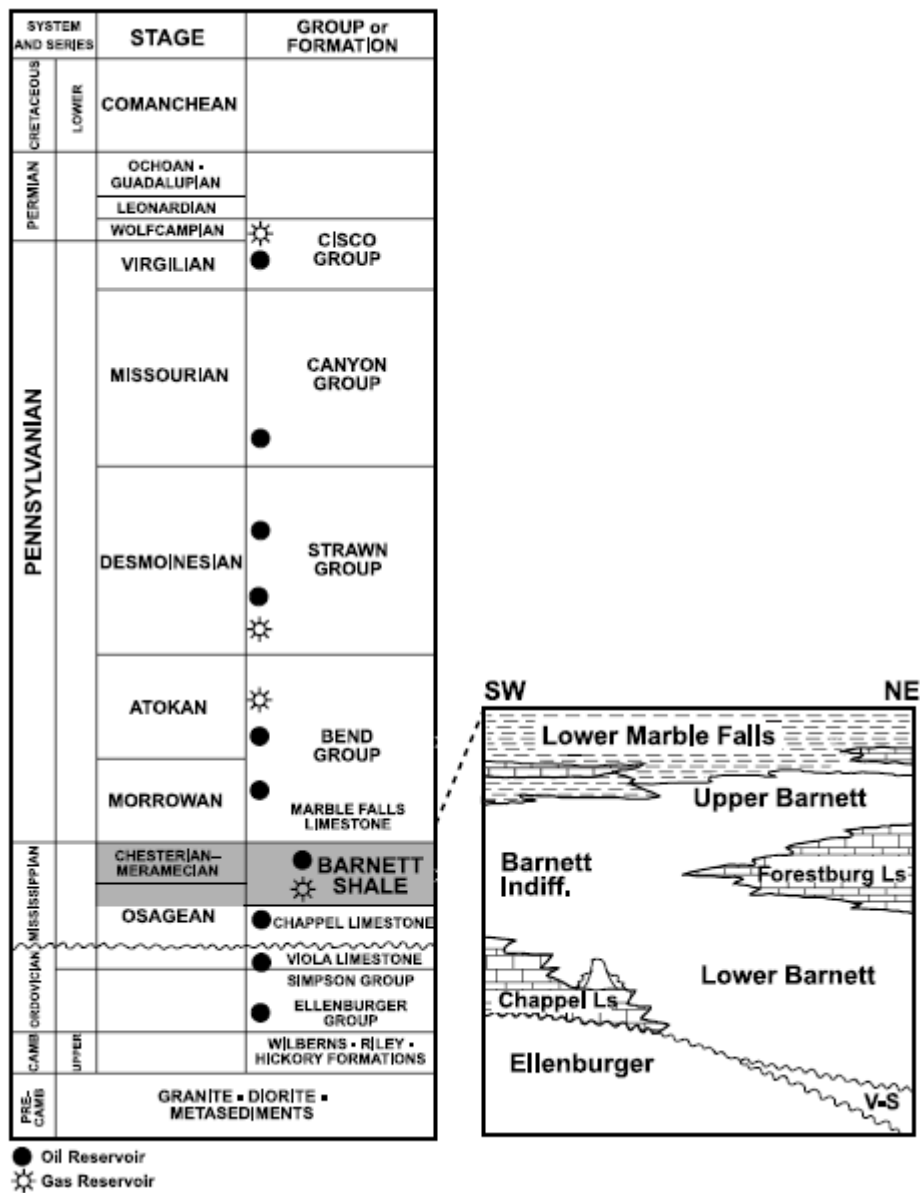


Figure 2.1- Generalized stratigraphic column, Fort Worth basin. Expanded section shows more detailed interpretation of Mississippian stratigraphy. V-S refers to Viola-Simpson interval (from Montgomery et al., 2005).

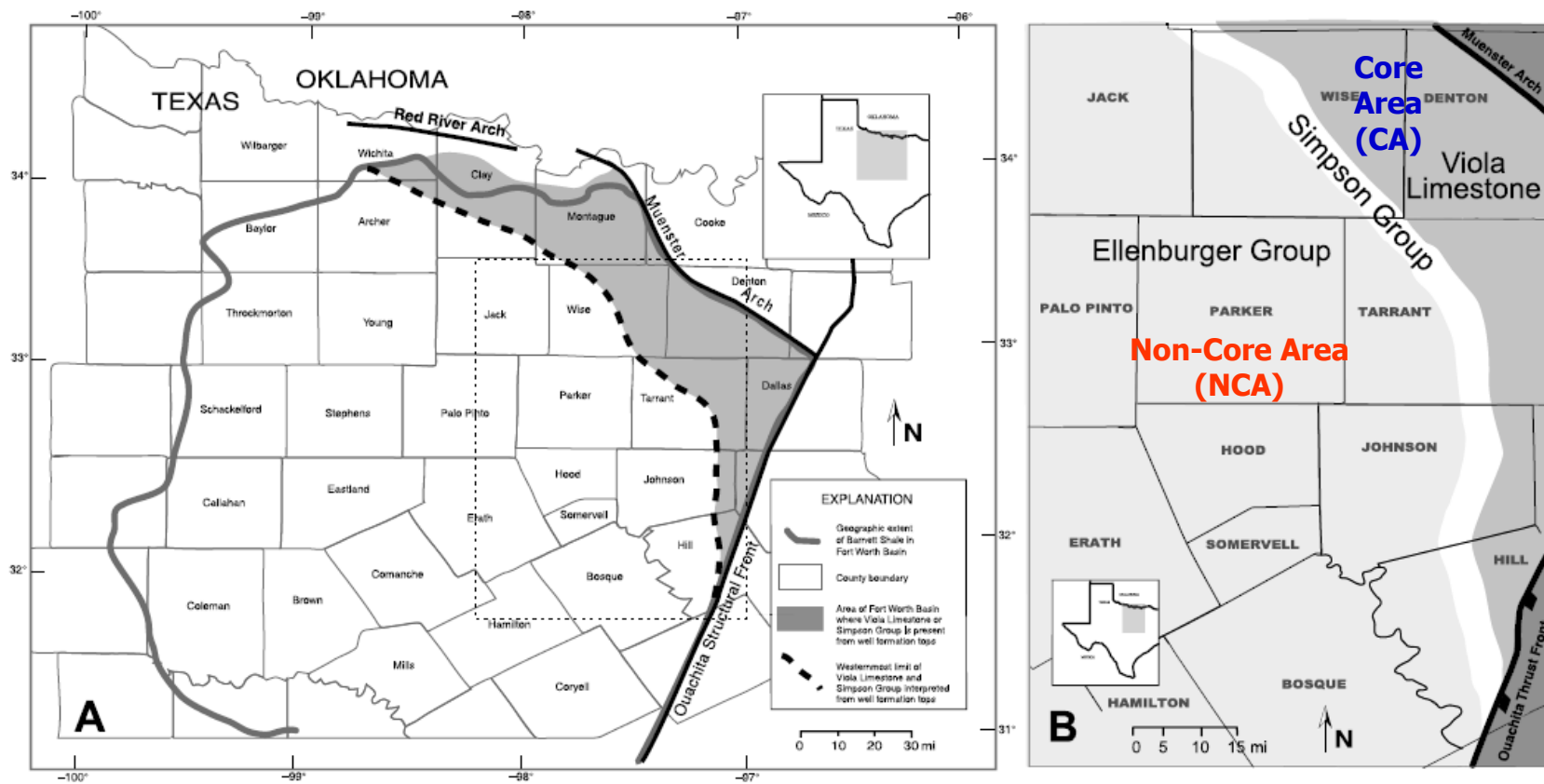


Figure 2.2– (A) Area determined where Viola Limestone or Simpson Group is present. Dotted rectangle represents area shown in (B). (B) Map showing subcrop geology of the Barnett Shale (modified from Pollastro et al., 2007).

Martineau (2007) identified five stages in the development of the Barnett shale play with regards to completion strategy; they include;

1. Drill a vertical well and fracture the lower Barnett with 150,000-300,000 gal of water based liquid usually nitrogen assisted, pumping rate was 40 barrels per minute.
2. Drill a vertical well and fracture the lower Barnett with 400,000 – 600,000 gal of cross-linked fracture fluid usually nitrogen assisted, pumping rate was 40 barrels per minute.
3. Drill a vertical well and fracture the upper and lower Barnett separately with 500,000 gal and 900,000 gal of water respectively, pumping rate was 50-70 barrels per minute.
4. Re-fracturing of previously gel-fractured wells with water.
5. Drill horizontal wells in the lower Barnett with laterals ranging from 1000 to 3500 ft fractured with 2,000,000 – 6,000,000 gals of water, pumping rate was 50-100 barrels per minute.

He also stated that the Barnett shale is over-pressured in the core area (0.54 psi/ft). Reservoir permeabilities in the Barnett Shale range from 0.00007 to 0.0005 md (milli-darcy).

2.2 General Analysis of Data from the Barnett Shale

As of December 31st, 2008, there were a total of 10,777 wells drilled to access reserves in the Barnett Shale. The distribution of these wells per county is shown in **Table 2.1**. Approximately 90% of deviated of the deviated and vertical wells exhibit continuous production of water as compared to 53% of the horizontal wells.

Table 2.1- DISTRIBUTION OF WELLS IN THE NON-CORE AND CORE COUNTIES OF THE BARNETT SHALE AS AT DECEMBER 31ST, 2008

	<u>Counties</u>	<u>Number of Wells</u>			<u>Number of water producing wells</u>		
		*D	**H	***V	*D	**H	***V
Non-Core Counties	Eastland	0	11	8	0	0	1
	Erath	0	121	18	0	33	13
	Hood	0	545	11	0	250	9
	Jack	0	92	55	0	51	43
	Palo Pinto	0	38	23	0	6	15
	Parker	6	864	159	4	483	129
	Somervell	0	46	0	0	21	0
	Bosque	0	9	0	0	5	0
Core Counties	Denton	156	758	1629	139	462	1533
	Johnson	10	2138	68	7	1113	43
	Tarrant	182	1478	291	166	765	265
	Wise	160	478	1423	141	282	1266

* 'D' means deviated, ** 'H' means horizontal , *** 'V' means vertical

For the purposes of clarity, most of the deviated wells are oriented vertically across the Barnett shale pay. **Fig. 2.3** shows a break-down of the wells in the Barnett Shale based on well type. These wells are usually stimulated using hydraulic fracturing. Water is usually the base for the stimulation fluid. We began our analysis of data from this province by plotting the cumulative gas production (Mcf) against cumulative water production (bbls) for completions in the unconventional reservoirs of the Barnett Shale (**Fig. 2.4**) and for completions in the conventional reservoirs of the Fort Worth Basin (**Fig. 2.5**). Based on visual inspection, there is little correlation between these parameters in both **Fig. 2.4 & Fig. 2.5**. However, as expected, vertical / horizontal wells drilled in

the core area of the Barnett shale are generally more productive than wells drilled in the non-core area (Figs. 2.6 and 2.7).

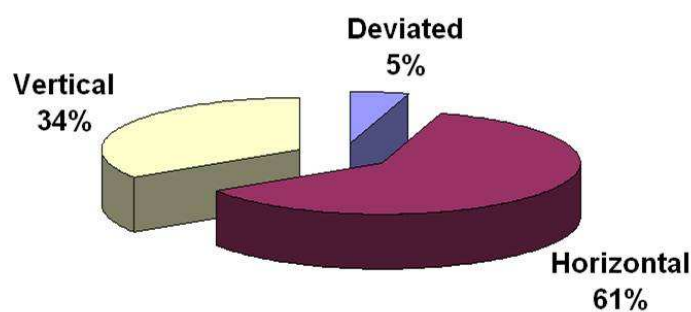


Figure 2.3– Percentage breakdown of wells in the Barnett Shale based on well type (data from HPDI).

This phenomenon is attributed to (1) greater thickness of the Barnett Shale in the core area, (2) greater Total Organic Carbon (TOC) and/or vitrinite reflectance in the core area and, (3) the presence of a fracture barrier between the shale and the underlying water bearing layer. We now look at average water and gas production data from the Barnett Shale on a county by county basis. We evaluate gas recovery from these completions using the cumulative gas produced normalized by the length of time the well has produced. For all of the statistical evaluation, we use the P50 value for the data under consideration. The P50 value of a variable is the value below which 50% of the observations may be found. The P50 value will serve as our measure of central tendency

or will represent the performance of the average well. We present an analysis of water and gas production data for deviated, vertical and horizontal wells in the Barnett Shale. In **Fig. 2.8A**, we see average gas production for deviated wells in the Barnett Shale.

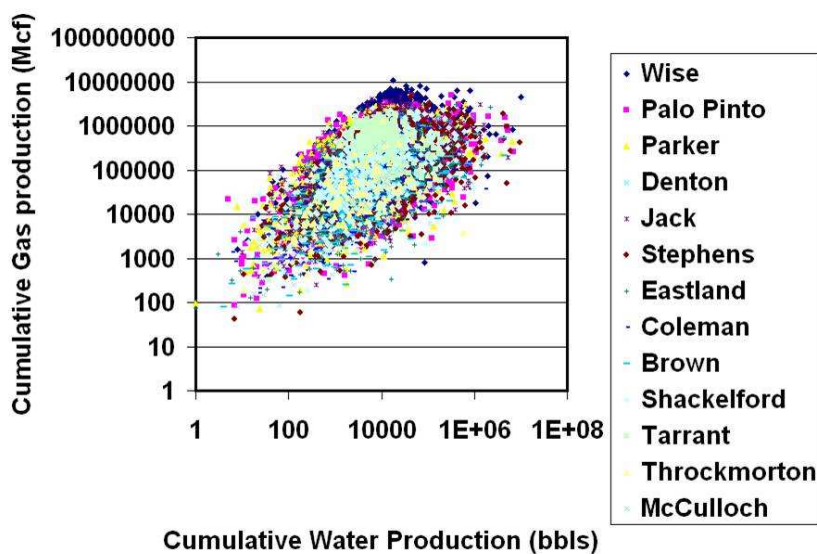


Figure 2.4– Relationship between cumulative gas and water production in conventional reservoirs of the Fort Worth basin.

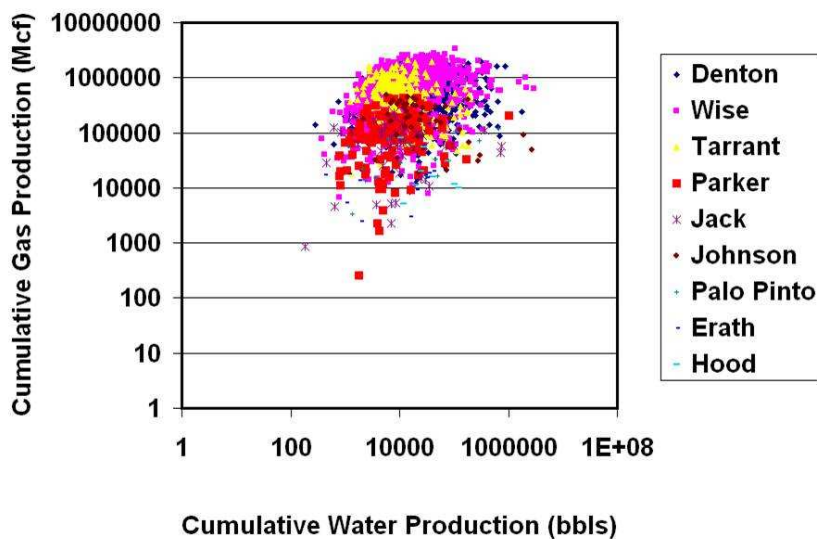


Figure 2.5– Relationship between cumulative gas and water production in unconventional reservoirs of the Fort Worth basin.

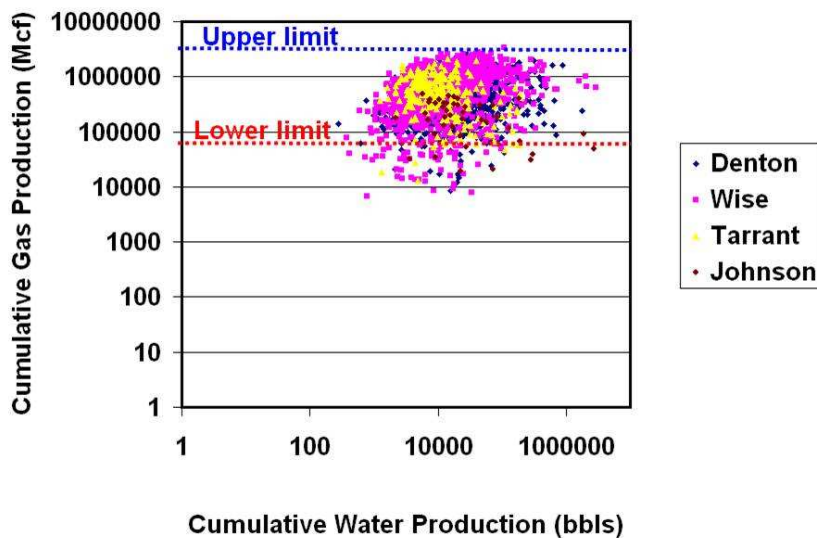


Figure 2.6– Relationship between cumulative gas and water production in Core Area of the Barnett Shale.

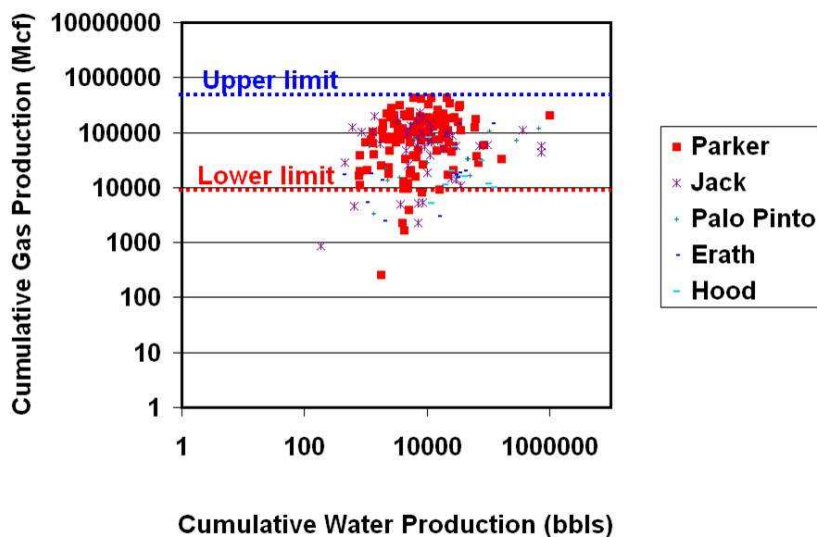


Figure 2.7– Relationship between cumulative gas and water production in Non-Core Area of the Barnett Shale.

Based on the data we have, deviated wells were drilled mainly in the Core Area of this gas province. In the same vein, **Fig. 2.8B** and **Fig. 2.8C** show average gas production for horizontal and vertical wells. We can conclude from these bar charts that

we have better gas production averages from counties in the Core Area of the Barnett Shale. This supports the notion that the location of a well in the Barnett Shale is a key predictor of productivity. **Figs. 2.9A, B&C** show average water production for completions in the Barnett shale. In **Fig. 2.9B**, we see that wells drilled in the Non-Core Area show little to no water production. This can be attributed to the use of horizontal wells and the careful design of hydraulic fracturing treatments to prevent unrestrained fracture height development. However, these water production trends do not necessarily translate to increased gas productivity when compared to wells in the Core Area. In **Fig. 2.9B**, Jack County in the Non-Core Area seems to have abnormally high water production. This goes against the trend in the Non-Core Area as stated above. However, most wells in the Jack county are older compared to other wells in the NCA. Therefore, it is possible the hydraulic fracturing treatments were more aggressive. Also for vertical wells, **Fig. 2.9C** supports the hypotheses that the average water production for counties in the NCA is smaller compared to average water production for counties in the CA. It is also worthy to note that Jack and more starkly, Hood counties buck the aforementioned trend. **Appendix A** contains the raw data from which these charts were constructed. However, for the purpose of clarity and subsequent analysis, **Tables 2.2A and 2.2B** show the average production data for Denton County (CA) and Parker County (NCA). We choose to highlight data from the Denton and Parker Counties because (1) they have good spread of deviated, vertical and horizontal wells and, (2) Geology can be considered to be consistent over the entire county, at least, on a macro-scale in the Core and Non-Core Area respectively.

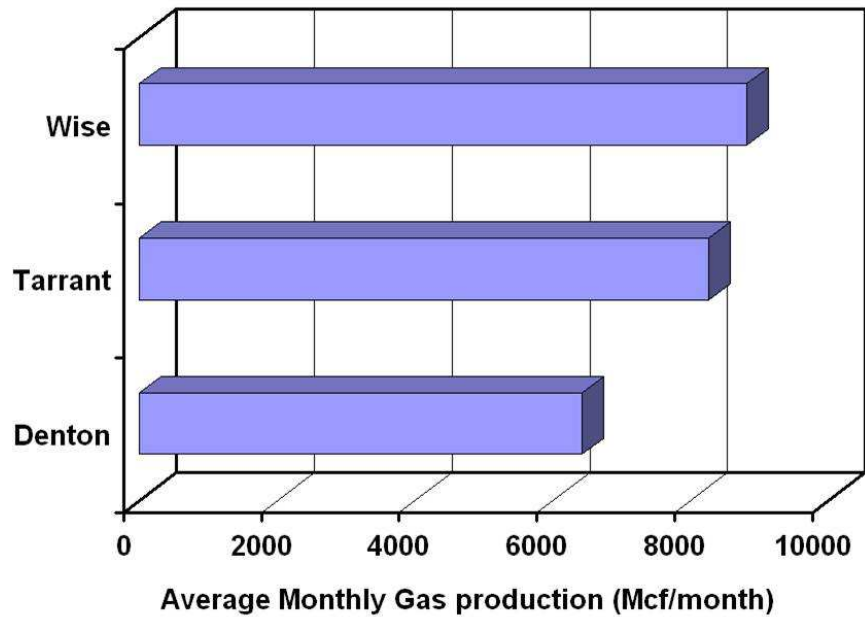


Figure 2.8A – P50 values for gas production (deviated wells).

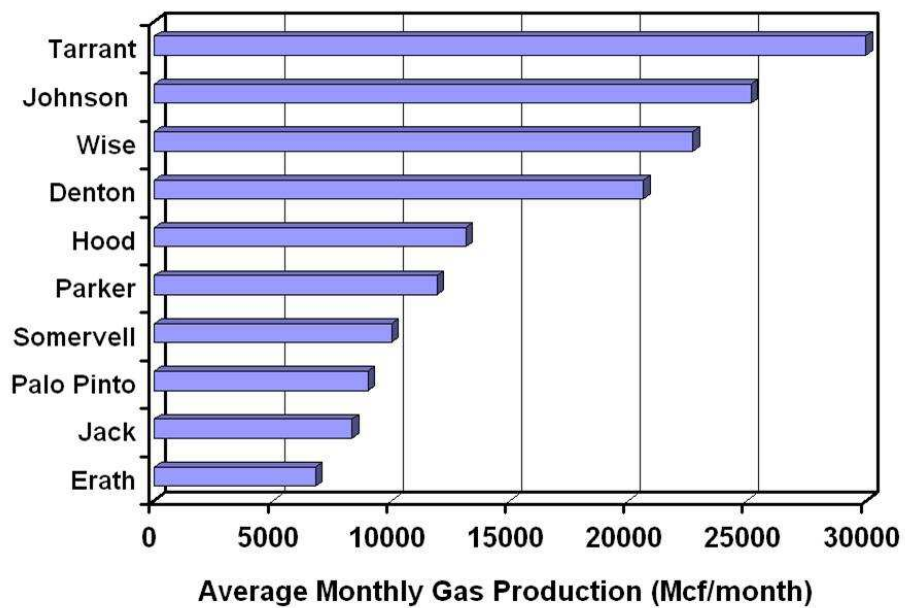


Figure 2.8B – P50 values for gas production (horizontal wells).

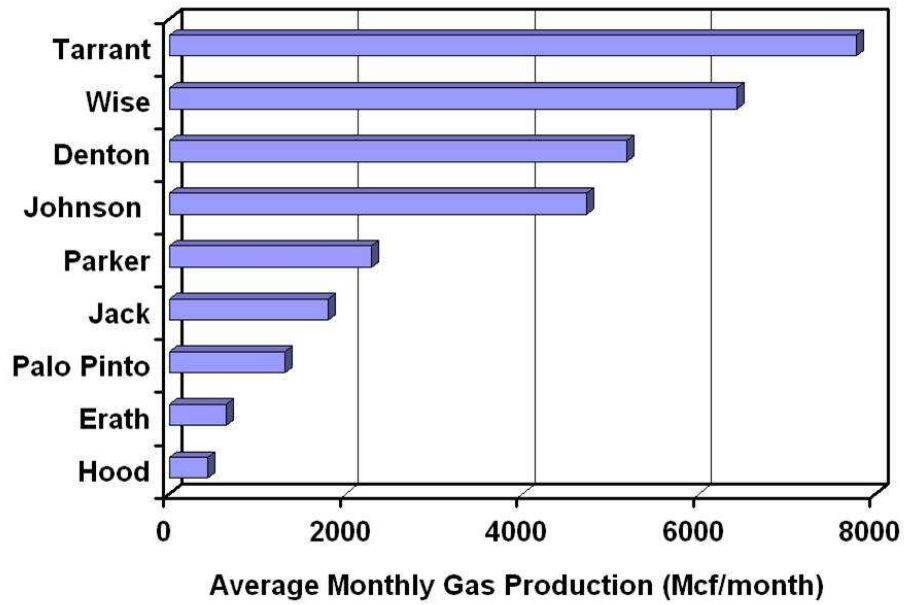


Figure 2.8C – P50 values for gas production (vertical wells).

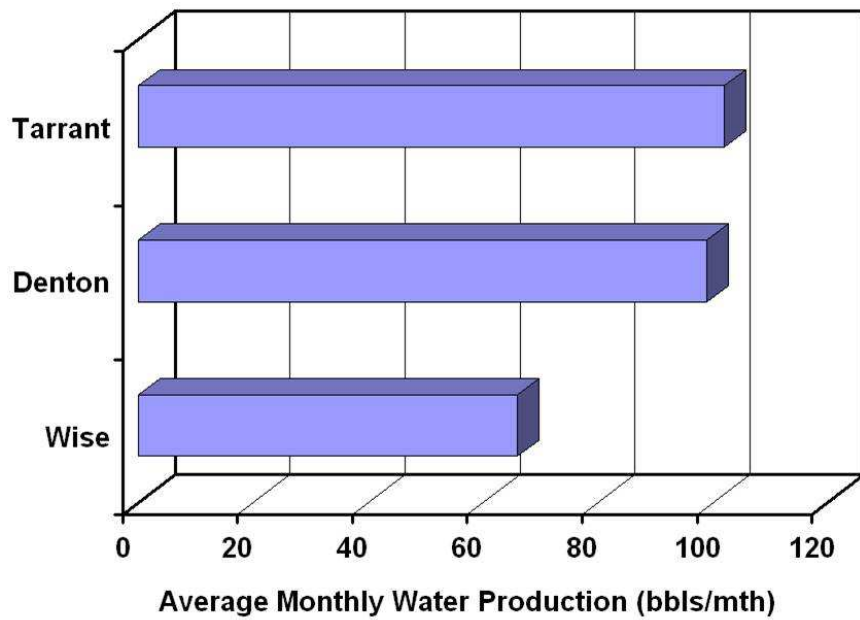


Figure 2.9A – P50 values for water production (deviated wells).

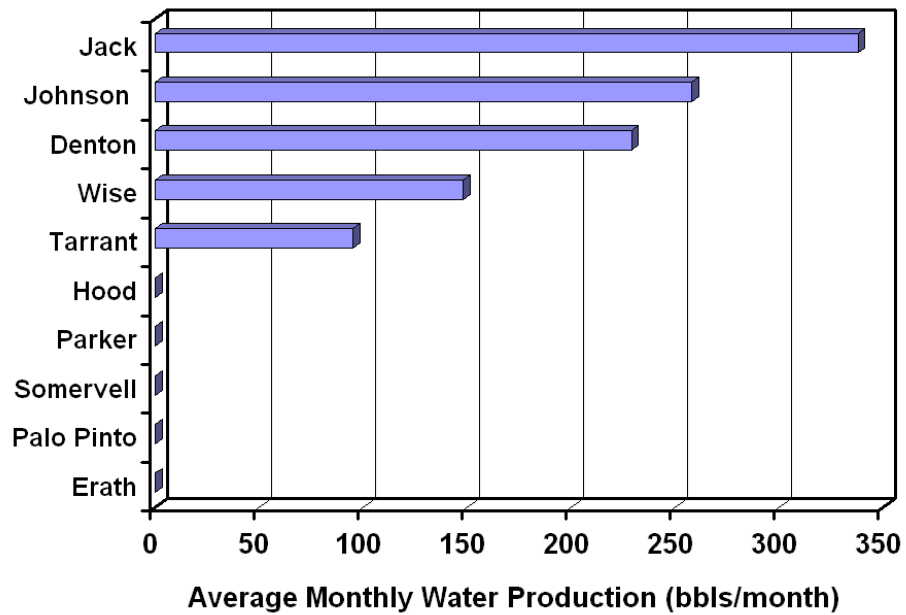


Figure 2.9B – P50 values for water production (horizontal wells).

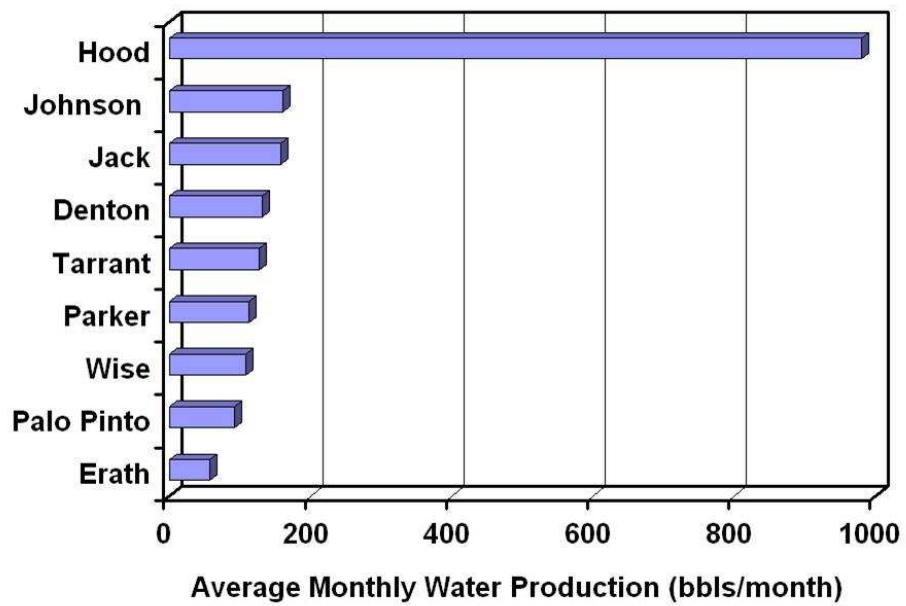


Figure 2.9C – P50 values for water production (vertical wells).

Table 2.2A – STATISTICAL ANALYSIS OF DATA FROM DENTON COUNTY

	<u>Gas (Mcf/mth)</u>			<u>Water (bbls/mth)</u>			<u>WHP (psi)</u>		
	<u>P10</u>	<u>P50</u>	<u>P90</u>	<u>P10</u>	<u>P50</u>	<u>P90</u>	<u>P10</u>	<u>P50</u>	<u>P90</u>
Deviated	3535	6427	11898	0	99	293	50	200	356
Horizontal	7053	20716	39689	0	229	1540	0	180	328
Vertical	2244	5184	10430	45	132	566	90	220	405

Table 2.2B – STATISTICAL ANALYSIS OF DATA FROM PARKER COUNTY

	<u>Gas (Mcf/mth)</u>			<u>Water (bbls/mth)</u>			<u>WHP (psi)</u>		
	<u>P10</u>	<u>P50</u>	<u>P90</u>	<u>P10</u>	<u>P50</u>	<u>P90</u>	<u>P10</u>	<u>P50</u>	<u>P90</u>
Horizontal	2986	11926	27712	0	0	4312	0	103	300
Vertical	424	2295	5165	0	112	704	0	150	400

Fig. 2.9B suggests that the average horizontal well in the Parker County produces minimal amount of water. This might as well be the case, but as seen in **Table 2.2A**, the P90 value for water production in Parker County is a lot higher than the P90 value for water production in Denton County. Another interesting data trend is reflected in the number of deviated, vertical and horizontal wells completed in the Barnett shale as a function of time (**Figs. 2.10 and 2.11**). This trend shows that horizontal wells are the completion of choice in the Barnett Shale as at present. An interesting question is the following; what is the most important predictor of gas well productivity in the Barnett Shale; is it time of completion / hydraulic fracturing technology or is it well location? **Figs 2.12 and 2.13** show that average gas productivity for the worst performing year (2005) in Denton County is the equivalent of the best performing year (2007) in Parker County. Therefore as expected, based on these data, location is a more important factor

than time of completion. We note that the time of completion will be related to the hydraulic fracturing technique used to stimulate the well.

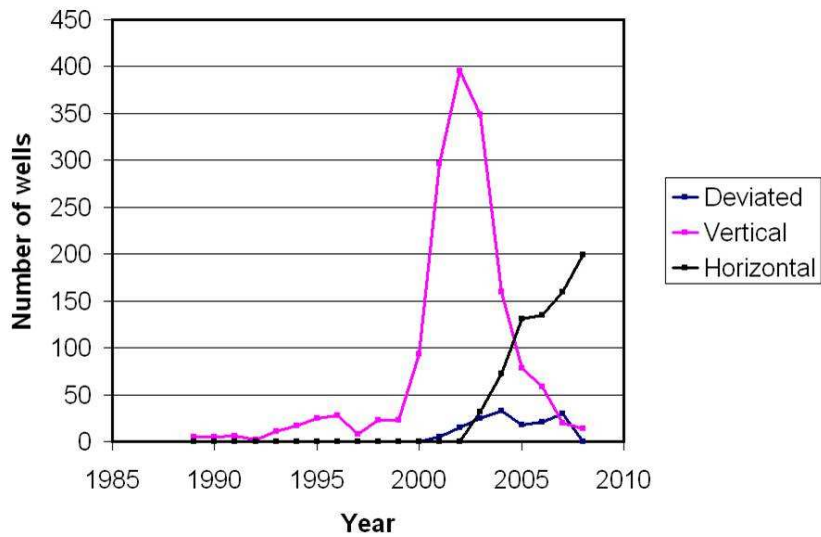


Figure 2.10- Number of wells completed in Denton County by type per year.

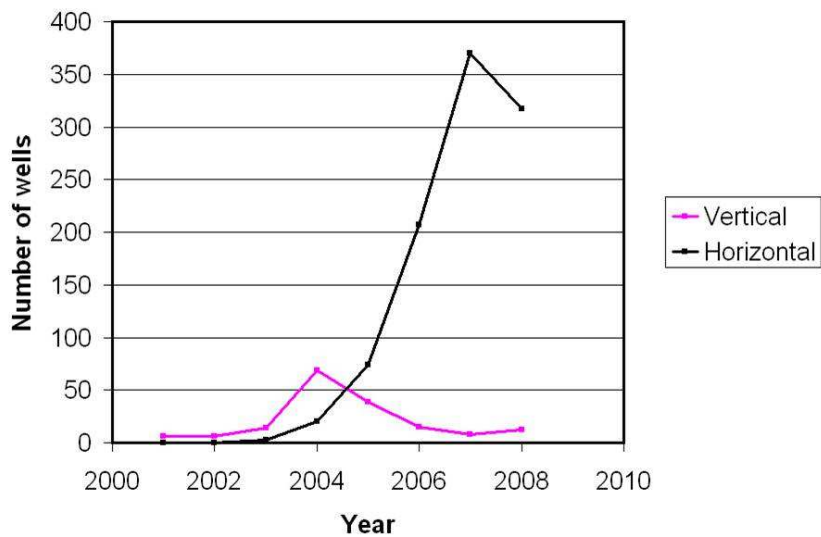


Figure 2.11 - Number of wells completed in Parker County by type per year.

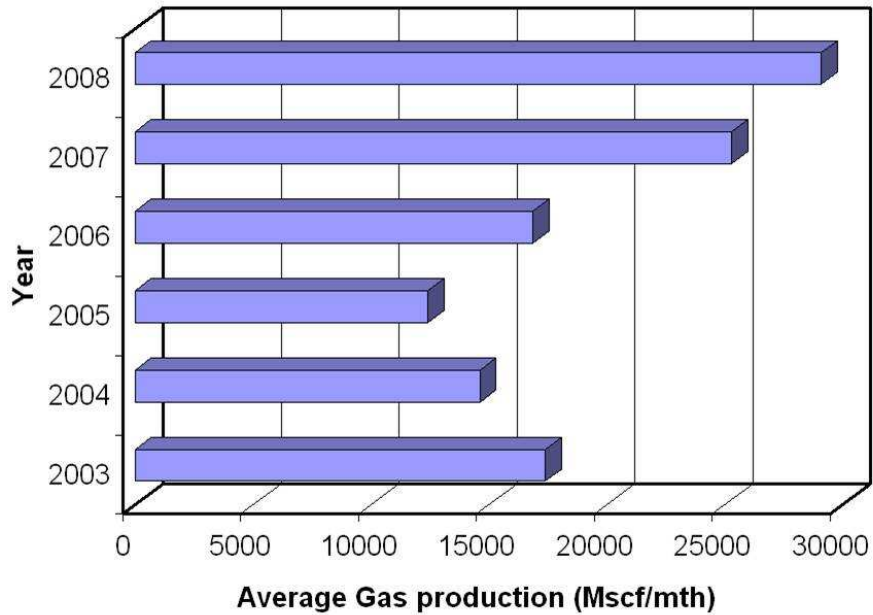


Figure 2.12 - P50 values for average gas production every year in Denton County (horizontal wells).

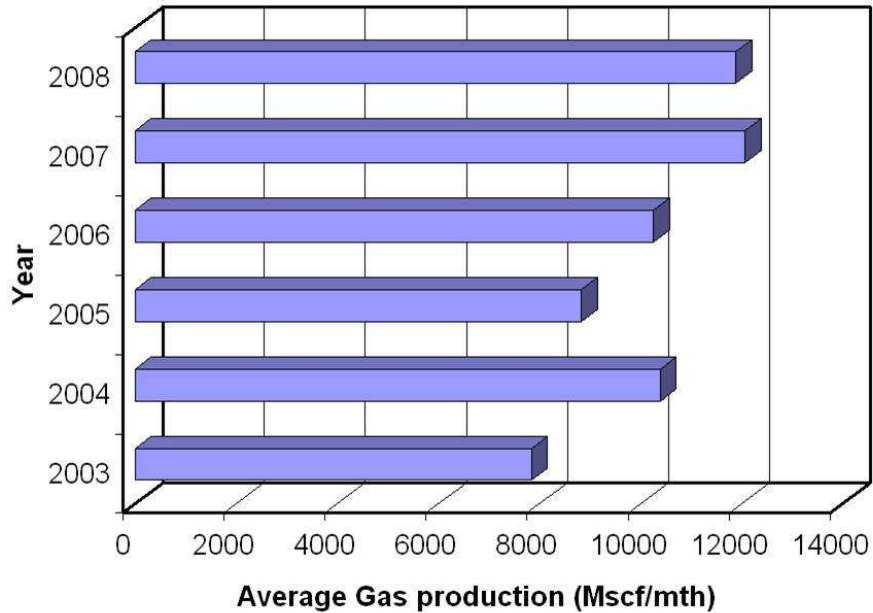


Figure 2.13- P50 values for average gas production every year in Parker County (horizontal wells).

It is also of interest to show that water production from both Denton and Parker Counties (Figs. 2.14 and 2.15) seem to decrease with time. This decrease can be a reflection of three possible factors; (a) reduced fracturing fluid volume (not likely) (b) more fracture

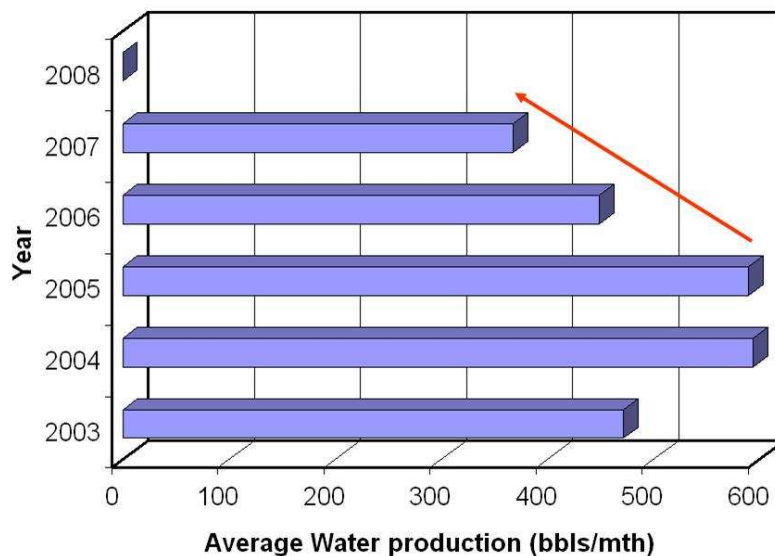


Figure 2.14 - P50 values for average water production every year in Denton County (horizontal wells).

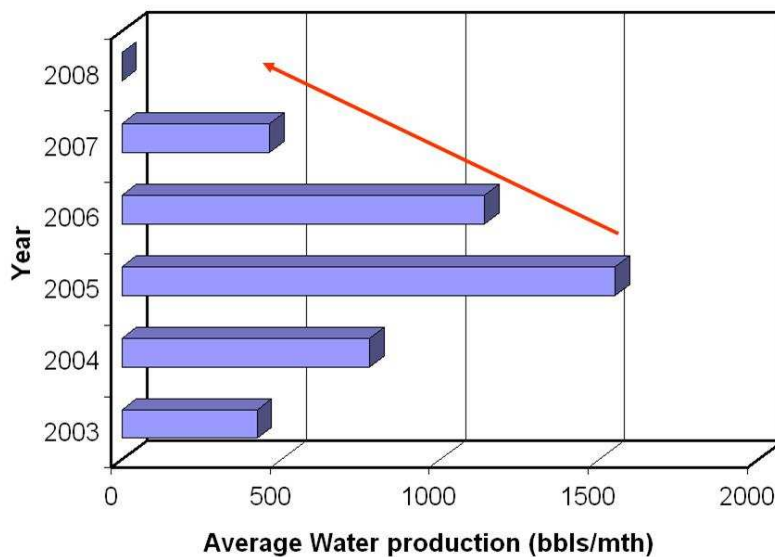


Figure 2.15 - P50 values for average water production every year in Parker County (horizontal wells).

fluid retention by the rock and, (c) the induced fractures do not propagate excessively and connect to the underlying Ellenburger formation.

We did not make detailed statistical analysis of reservoir parameters like the Barnett Shale pay thickness or the thickness of the fracture barriers. This is because these data were not available for these wells especially in a spatial sense. These kinds of data are usually part of the records kept by operating companies. We tried to request access to these data, but we had no success.

2.3 Effect of Water Production on Gas Well Productivity

Given the water production characteristics of the Barnett shale wells seen in the previous section, we decided to ascertain whether liquid loading had the potential to limit gas well productivity in this shale province. **Table 2.3** shows the data we used to investigate this phenomenon. These data reflect to the best of our ability the actual conditions prevailing in the Barnett Shale.

Table 2.3– PARAMETERS USED TO INVESTIGATE LIQUID LOADING IN THE BARNETT SHALE

<u>Parameter</u>	<u>Value</u>
Ω , interfacial tension (dynes/cm)	60
ρ_L , density of water (lbs/cu.ft)	67
Specific gravity of gas	0.6
Wellhead Flowing temperature (Rankine)	580
Wellhead Flowing pressure (psi)	200-2200
Flow area of conduit (sq.ft), for 2.375" tubing	0.021708

We used equations developed by Turner et al. (1969) to develop a graph of wellhead pressure versus the minimum flow rate required to prevent liquid loading as shown in **Fig. 2.16**. The data used to construct this figure shows that the average vertical well in Denton and Parker counties of the Barnett Shale currently experience liquid loading. For horizontal wells, because of the higher gas rates, liquid loading is less important especially in the CA. We would like to note that though liquid loading is a less important phenomenon in horizontal completions, some of the horizontal wells in the NCA produce at relatively low rates and might therefore be susceptible to liquid loading. Also, the Turner equations do not take into consideration well deviation. Therefore, it is likely that the average horizontal well in Parker County is also susceptible to liquid loading, given the close proximity of its plotted data point to the liquid loading region.

In the last section, we reviewed literature pertaining to the effect of load-water on gas well productivity in gas shales. We would like to note that the references based their conclusions on the simulation of wells in tight gas reservoir models. Tight gas reservoirs are not analogous to shale gas reservoirs. In a general reservoir engineering sense, capillary pressure curves used for tight gas reservoirs might not be applicable to shale gas reservoirs.

Also, specific to the Barnett Shale, all these simulations failed to consider the effect of an 'external water source' like the Ellenburger formation. Therefore, the conclusion that water production does not have long term deleterious effect on gas well productivity in tight gas sands should only be applied to shale gas systems in light of these limitations.

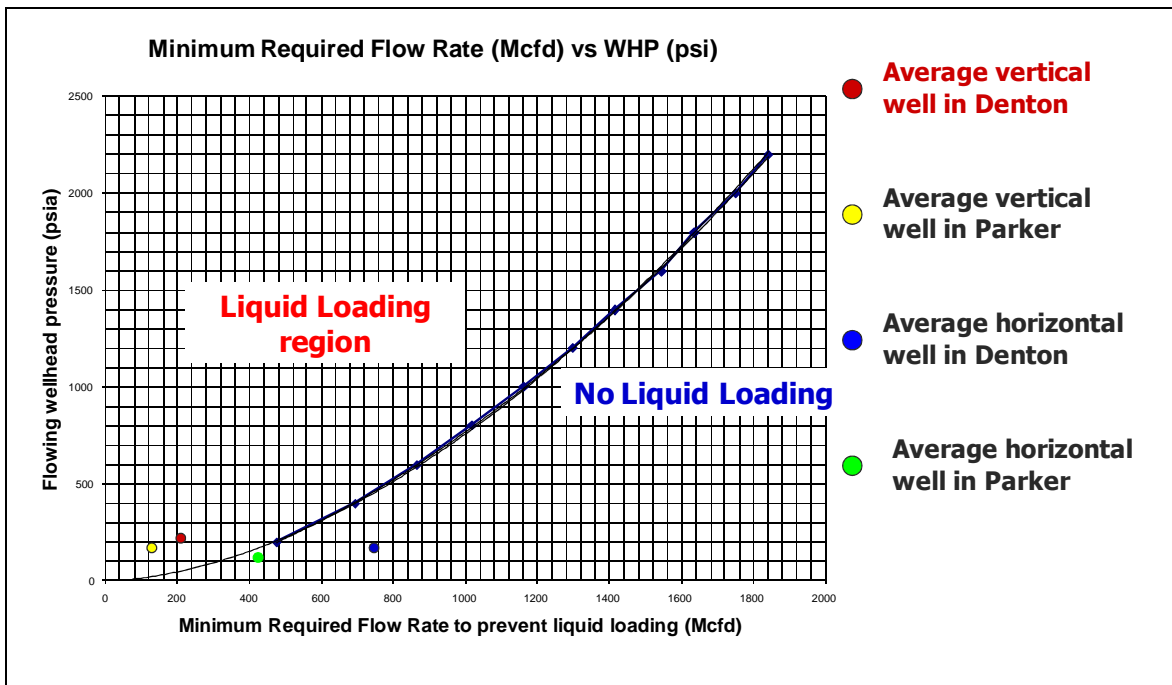


Figure 2.16– Predictive Chart for onset of liquid loading in the Barnett Shale.

2.4 Section Summary

Based on the data analyzed, we conclude the following:

- In general, wells in the Core Area of the Barnett Shale are better producers. For wells with the same completion type, location is more important than time of completion or hydraulic fracturing strategy. If time of completion or hydraulic fracturing strategy was more important, one would expect more recent wells to have better productivity more regardless of location.
- On the average, wells in the Non-Core area of the Barnett Shale produce less water.
- The average vertical well in Denton and Parker Counties of the Barnett Shale currently experience liquid loading. Because the Turner equations do not take into

consideration well deviation, it is likely that the average horizontal well in Parker County or even Denton County is also susceptible to liquid loading.

3 ANALYSIS OF WATER PRODUCTION MECHANISMS IN THE BARNETT SHALE

3.1 Water-Hydrocarbon Ratio and Water-Hydrocarbon Ratio Derivative Analysis in Conventional Reservoirs

Using reservoir simulation models of a conventional reservoir, Chan (1995) discovered that the Water-Hydrocarbon ratio and the derivative of the Water-Hydrocarbon ratio show characteristic signatures depending on the water producing mechanism. **Figs. 3.1A, B & C**, reproduced from Chan's paper, summarize his findings.

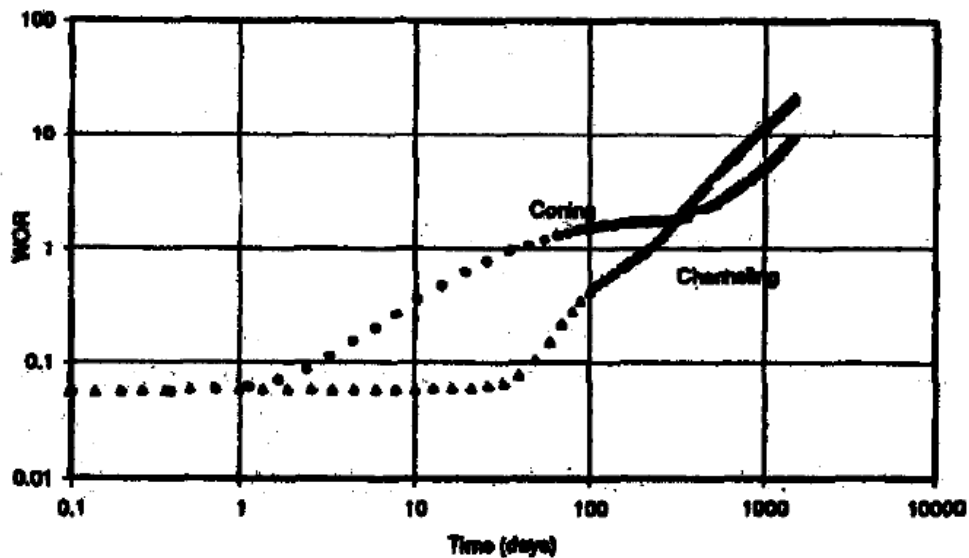


Figure 3.1A – Water coning and channeling WOR comparison plot.

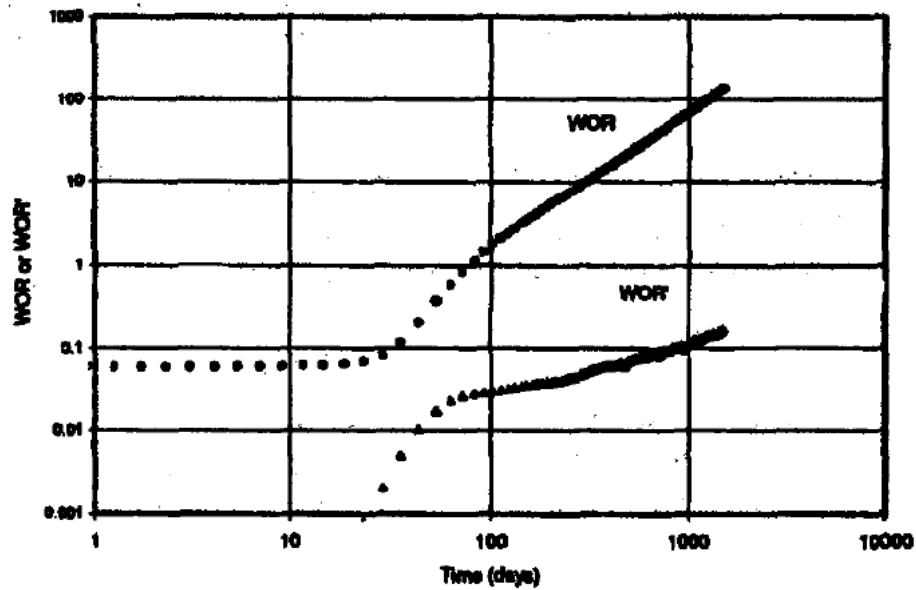


Figure 3.1B – Multi-layer channeling WOR and WOR derivative plot.

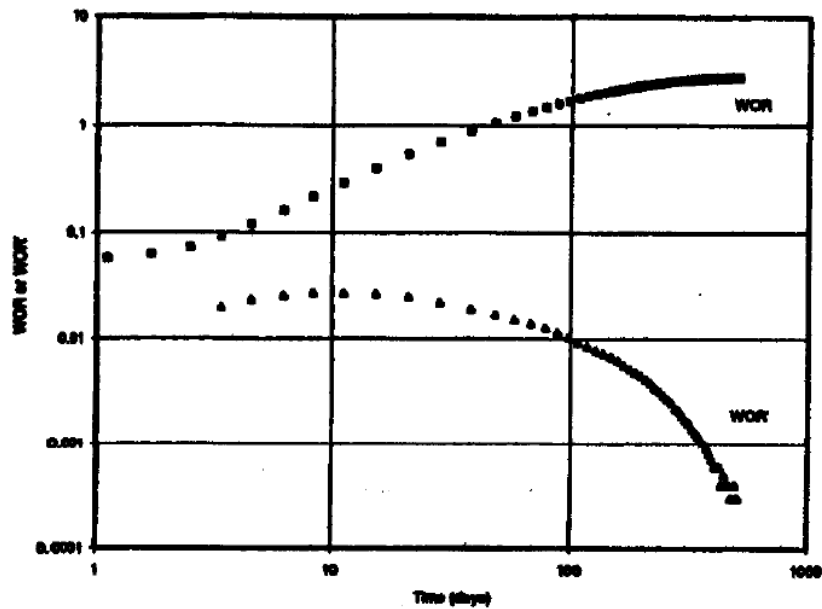


Figure 3.1C – Bottom water coning WOR and WOR derivative plot.

Seright (1997) determined that these curves are not unique. We agree with Seright, only with the caveat that the curves proposed by Chan are still useful as an initial

screening tool. They can also offer insight into the likely source of water production from an interval when used in conjunction with other tools.

3.2 Water-Hydrocarbon Ratio and Water-Hydrocarbon Ratio Derivative Analysis in Unconventional Reservoirs

Chan applied his diagnostic plots to production data from conventional reservoirs. The main mechanisms of water production assuming wellbore integrity was coning and channeling. We decided to apply his methodology to the production data we have from the Barnett shale. It is logical to assume that it is not likely water coning would be a significant mechanism in gas shales because of the ultra-low permeabilities encountered. Therefore, the most logical mechanism of water production apart from load water would be channeling. In this case, we refer to small fractures connecting the main hydraulic fracture to an underground water bearing layer and / or karst. Wellbore integrity is also assumed. Specifically for the Barnett shale, we anticipate that there will be the following sources of water:

1. Load water
2. Underlying water bearing layer – Ellenburger formation
3. Water bearing layers in gross shale as reported in literature

However, our analysis of water production data from the Barnett shale might be compromised because some of the data might be allocated values based on a constant WGR. With this limitation in mind, we will present a conceptual framework to explain the WGR and WGR' behavior seen in the data analyzed. This framework is hypothetical and will be subject to further refinement or overhaul. One characteristic we notice while analyzing water and gas production data from the Barnett shale was that water production

increase did not necessarily accompany gas production decrease as might be suggested by classical relative permeability theory. This might suggest both water and gas flow through different pathways with possibly different depletion mechanisms. An alternative explanation for this trend is if water production was computed by applying a constant WGR to gas production data. **Figs 3.2A, B, C & D** summarizes our understanding of the data analyzed. We think **Fig. 3.2A** represents the period of water production after the fracturing treatment, that is, after gas rate stabilization. This period is identified by a constant WGR. The length of this period is determined by the amount of liquid pumped into the reservoir and the effect of factors like external water sources, reservoir depletion and liquid loading.

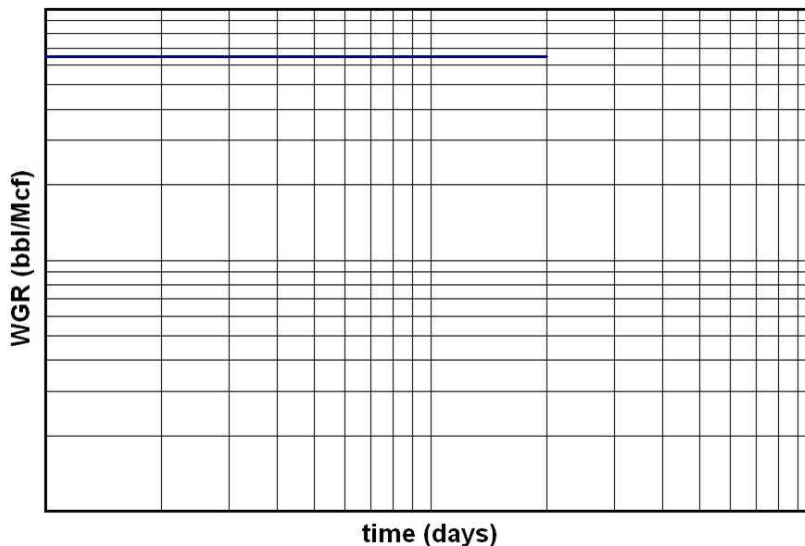


Figure 3.2A – WGR plots in Barnett Shale (Type 1).

We think **Fig. 3.2B** represents a period of either pressure depletion or liquid loading. This leads to a drop in WGR. The drop we have seen in WGR data from the Barnett shale is analogous to a shock front. One would think that the WGR decrease

would be gradual and approximate a smooth function. This abruptness may be due to allocated data or it may be due to gas displacement of water in a channelized network of fractures in an unconventional reservoir.

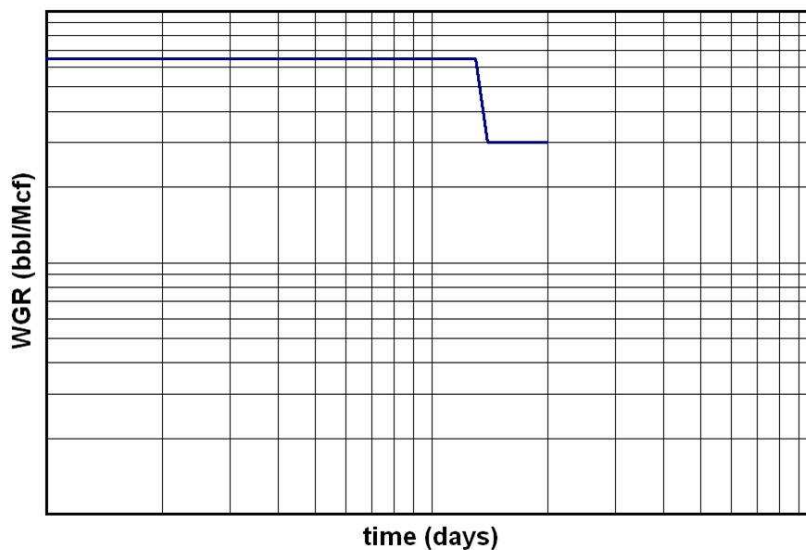


Figure 3.2B – WGR plots in Barnett Shale (Type 2).

We contend that if a sudden increase in WGR is seen from initial stabilized conditions especially for a reasonable period of production, this would be most likely due to an external source of water (**Fig.3.2C**). If we assume that the production pathways for water and gas are different, a sudden increase in water production is not likely to be related to relative permeability effects. Lastly, we noticed some wells in which some part of the WGR trend was analogous to repeating rectangular functions. We attribute this period especially when associated to oscillatory gas production behavior to liquid loading. Dousi et al. (2003) presented reasoning for understanding the process of liquid loading. Solomon et al. (2008) adapted their explanation and used **Fig. 3.3** to illustrate the process.

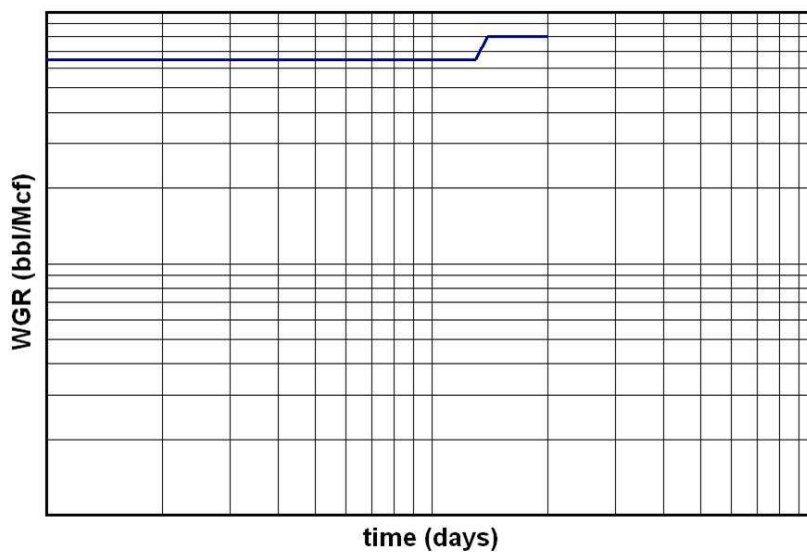


Figure 3.2C – WGR plots in Barnett Shale (Type 3).

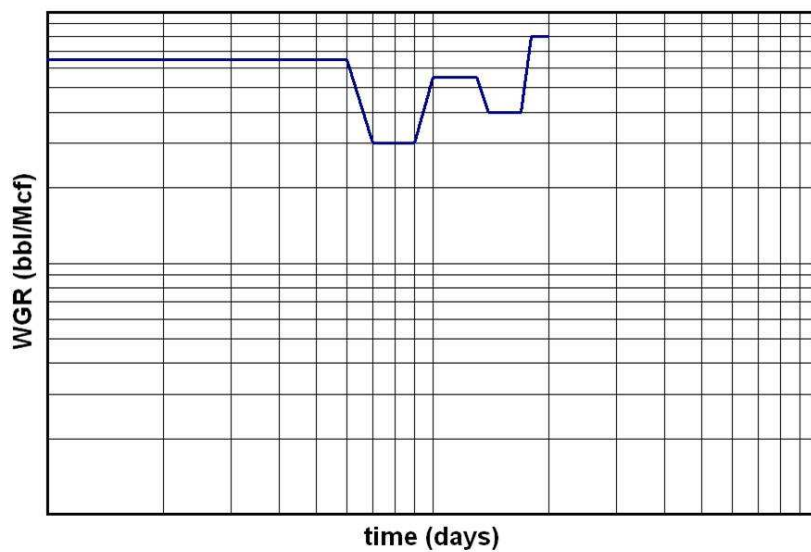


Figure 3.2D – WGR plots in Barnett Shale (Type 4).

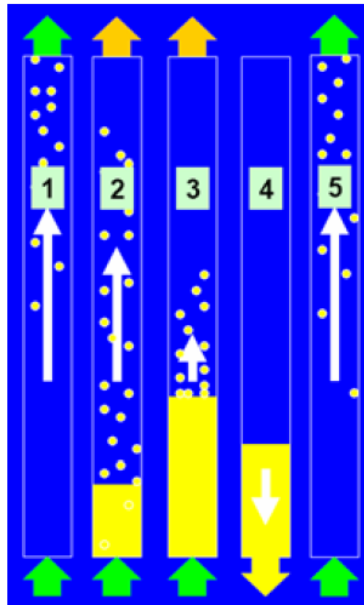


Figure 3.3– Liquid loading mechanisms description.

3.3 Load Water Recovery Factor in Denton and Parker Counties of the Barnett Shale

Figs. 3.4 A, B & C show the cumulative distribution function (CDF) for load water recovery factor in deviated, horizontal and vertical wells in the Denton County (representing the Core Area) of the Barnett Shale respectively. Also, **Figs. 3.5A & B** show the CDF for load water recovery factor in Parker County (representing the Non-Core Area) of the Barnett Shale. We define the Load Recovery Factor (LRF) as the ratio of the cumulative water produced to the fracturing treatment volume. **Fig. 3.4A** implies that most deviated wells do not produce back all of the load water. This conclusion is drawn based on the sample analyzed and might not generalize. However, approximately 15% of the vertical and horizontal wells in the Denton County have LRF's >1 (**Figs. 3.4**

B&C). Also, 15% / 35 % of the horizontal / vertical wells respectively in the Parker County produce with a LRF>1 (**Figs. 3.5A&B**).

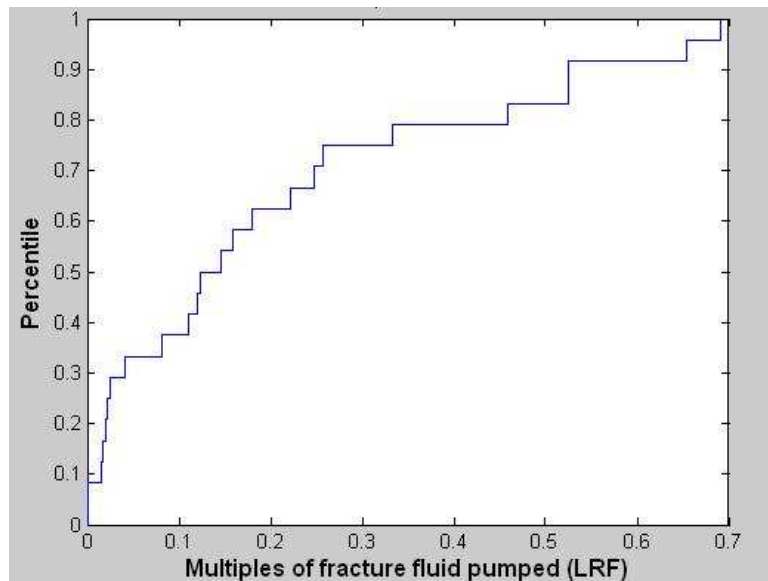


Figure 3.4A – CDF plot of Load Recovery Factor (LRF) for deviated wells in Denton County.

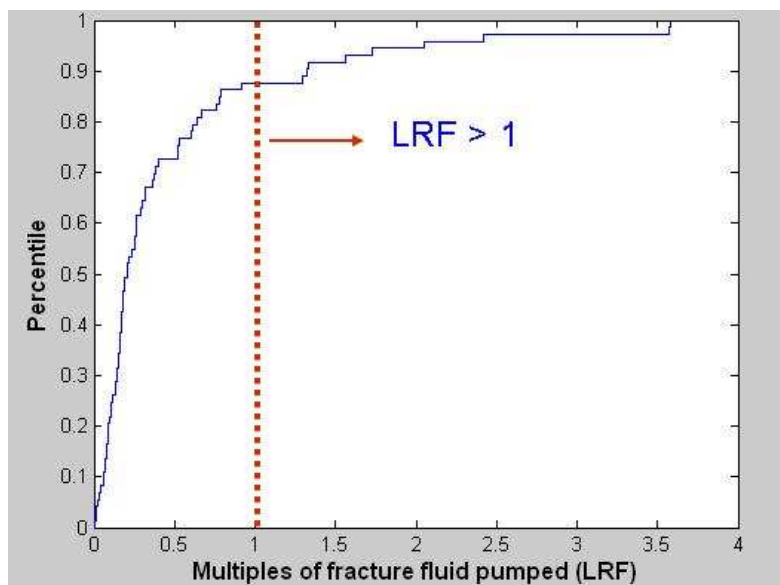


Figure 3.4B– CDF plot of Load Recovery Factor (LRF) for horizontal wells in Denton County.

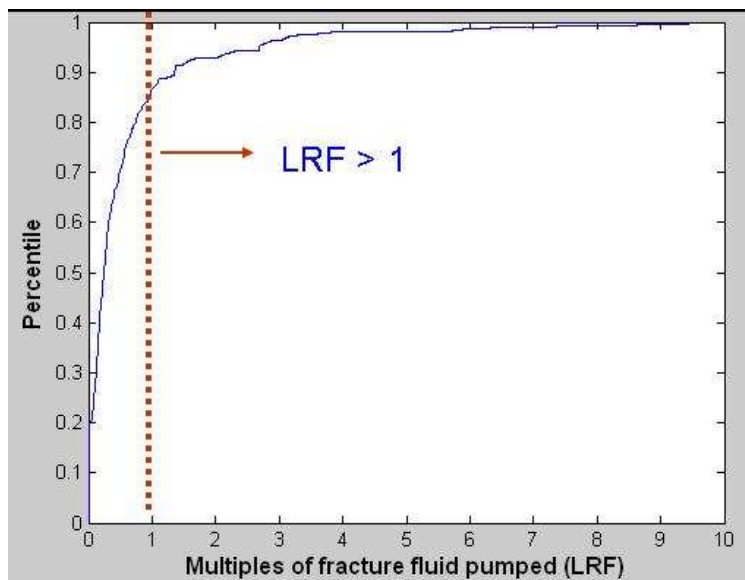


Figure 3.4C – CDF plot of Load Recovery Factor (LRF) for vertical wells in Denton County.

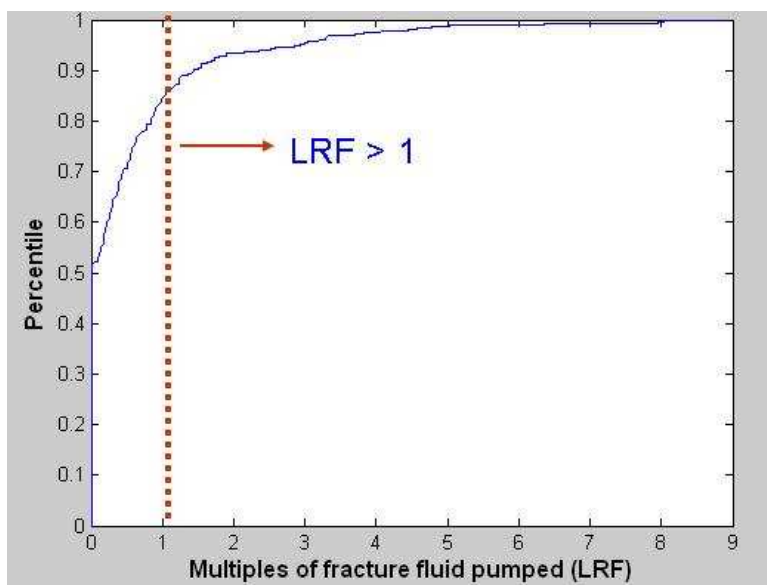


Figure 3.5A – CDF plot of Load Recovery Factor (LRF) for horizontal wells in Parker County.

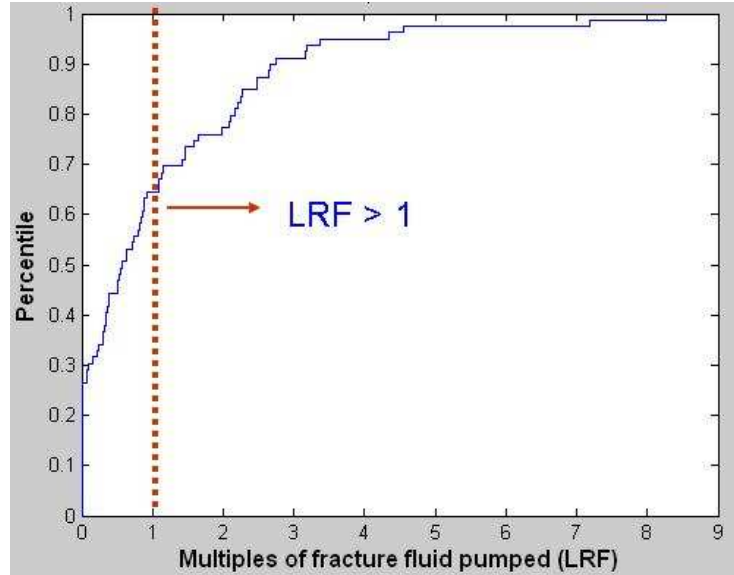


Figure 3.5B – CDF plot of Load Recovery Factor (LRF) for vertical wells in Parker County.

3.4 Section Summary

We achieved the following in this section:

- Reviewed previous work on the use of diagnostic plots in the production data analysis of conventional reservoirs.
- Developed a hypothesis to explain the WGR behavior of wells producing from unconventional reservoirs.

4 PRODUCTION DATA ANALYSIS USING NEURAL NETWORKS

4.1 Introduction

This section describes the use of neural network (NN) theory to estimate water production from a new well given certain well and hydraulic fracturing parameters. As shown from the literature review in Section 1, neural networks have been used to decipher non-linear relationships between variables in almost all facets of petroleum engineering. However, the use of this technique still remains controversial, especially for petroleum engineers. This is because the architectural design of a neural network to solve a problem is still essentially an art-form. There is a lot of uncertainty regarding the determination of the most relevant input vectors, the choice of the type of network architecture, the size of the network (number of layers), the connectivity between neurons and the number of neurons in each layer. In some problem domains, there is also a lot of concern as to whether the results from neural network runs honor the underlying physics of the problem.

However, for challenges that involve complex relationships between various disparate variables, neural network – based tools offer another way, or sometimes the only way, of deciphering these relationships. As a part of this section, we will look at the philosophical and statistical justifications for the use of machine learning and neural networks. Finally, we will describe the design and implementation of a neural network system used to predict average water production in the Denton County of the Barnett Shale.

4.2 Machine Learning Concepts

The discipline of machine learning involves the investigating how computers learn. This invariably means the study of classes of learning problems and algorithms. Since these problems are drawn from disparate domains, machine learning is an interdisciplinary field and it builds on the work of researchers from computer science, statistics, philosophy, psychology, neuro-sciences and engineering. There are many challenges in petroleum engineering that require the use of machine learning. Petroleum engineering is both a model and data intensive discipline. We use models that are based on our understanding of a physical process and solve these models using either analytical or numerical means. However, since most of our best models are developed under restricting assumptions, they do not generalize to all scenarios that might be encountered in real life. Also, because of improvements in computing and digital technology, a lot of well monitoring data is collected in real time. What would be the use of all these data if they cannot be used as a basis for further understanding of the systems which we operate? Hence, it is our opinion that machine learning will become a more important part of a petroleum engineers' toolbox because we need to improve our models. This is especially true in scenarios where data is not scarce. We will look at certain machine learning concepts and connect them to the problem at hand, which is, the prediction of average water production from an unconventional reservoir using well and hydraulic fracturing parameters. All the machine learning concepts described in this work are from Mitchell (1997) and Haykin (2005).

A Well-Defined Learning Problem – A learning problem is said to be well-defined if we can identify the following features.

1. The class of tasks
2. The measure of performance to be improved
3. The source of experience.

Learning is defined as the process by which a computer program improves its performance at some task through experience. Therefore, learner refers to the computing paradigm or algorithm by which learning is accomplished. Specifically, in our case, the task is to predict average water production from a new well drilled in an unconventional reservoir. The measure of performance is the accuracy of the prediction when compared to actual water production values. This implies we have to do some type of error analysis on the results from the learner. The source of the training information is from public databases.

Machine learning as function approximation – Petroleum engineers are quite familiar with the concept of function approximation. It is quite common-place to utilize linear regression techniques to find a polynomial fit relating input and output variables. However, if regression techniques fail to provide acceptable solutions to problems from certain domains because of their inherent non-linearity and complexity, machine learning paradigms can be used to approximate the relationship between input and output variables. For this case, we use neural networks as proxy for the function approximator. **Fig. 4.1** shows the input and output vector for the neural network. The function, f , is approximated by the neural network. The output of the neural network is the LHS while the input to the neural network is the RHS.

$$[\text{average well } q_w] = f \left[\begin{array}{c} \text{well location} \\ \text{Gas production rate} \\ \text{Barrier thickness} \\ \text{Interval thickness} \\ \text{Fracturing fluid volume} \\ \text{Proppant quantity} \\ \text{Well Type} \\ \text{Tubing / Casing depth} \\ \text{Tubing / Casing Size} \\ \text{Number of fracture stages} \\ \text{Gas specific gravity} \\ \text{Number of months produced} \\ \text{Acid pumped or not} \end{array} \right]$$

Figure 4.1– Neural network as a function approximator, f between input and output parameters.

Machine learning as hypotheses space search – machine learning can also be seen as a search in hypotheses space for a hypotheses that best matches the data. In this work, the tunable parameters are the weights of the neural network connections. The magnitude of these weights is varied to map the input and output parameters. This implies the hypotheses space of neural networks is actually infinite because each weight can take on infinite values.

Inductive bias in machine learning – The fundamental assumption upon which most machine learning algorithms are based is the Inductive Learning hypotheses. Informally, it states that “any hypotheses found to approximate the target function well over a sufficiently large set of training examples will also approximate the target function well over unobserved examples” (Mitchell, 1997). The caveat is that both the training

sample and test examples should come from a population with similar statistics. In this work, the case for using the inductive learning hypotheses is that the primary production drivers for wells in the Core Area of the Barnett Shale are comparable. Therefore, a neural network trained using data from Denton County in the Barnett Shale can approximate the water production potential from other wells drilled in other areas of Denton County or other areas of the Barnett Shale.

Machine Learning and Occam's razor – one of the forms of Occam's razor is as follows, “prefer the simplest hypotheses that fits the data” (Mitchell, 1997). There is a lot of argument as to the validity of the logic behind the above expression, but an exposition on these arguments is not our aim. In order to build a generalizable neural network, we chose the simplest network architecture and topology with the best performance given that data available. Performance would be evaluated over training, validation and test data sets. A more complex network would fit better with the training dataset but might fit test or validation datasets poorly. To reduce the chances of fitting the noise in our dataset, we would use the philosophy behind Occam's razor as one of our justifications for using the simplest network possible; hereby striking a balance between accuracy and generalization.

Learning Paradigms - There are two main types of learning paradigms. They are (1) Learning with a teacher or supervised learning (2) Learning without a teacher (reinforcement learning or self-organized learning). In supervised learning, the teacher has knowledge of the physical system in the form of input-output data pairs (labeled data, input is labeled to an output). For neural networks, the learning process is as follows; A training vector is applied to the neural network. The response of the neural network is

measured against the desired output. The network parameters (weights) are adjusted such that the neural network emulates the teacher. The main goal of this kind of network is to minimize a cost function that is related to true error surface averaged over all the input-output examples. Therefore, given an algorithm that can minimize the cost function, an adequate set of input-output examples and ample training time, a supervised learning system is usually able to approximate a highly non-linear function. We used average water production data from public databases as the teacher. Learning without a teacher can either be reinforcement learning or unsupervised/self-organized learning. However, in summary, for both paradigms, there is no teacher to oversee the learning process. The algorithm usually optimizes the free parameters of the network. Once the network has learnt the statistical nature of the input data, it has developed the ability to form internal representations that encode features of the input and create new classes automatically.

4.3 Neural Network Theory

The discussion above centered on machine learning theory, with some allusions to the application of neural networks. Neural networks are one of the tools used by machine learning researchers for function approximation. In this section, we will summarize neural network theory. This summary is based on the work of Haykin (2005). Neural networks have some interesting properties that are central to their use for machine learning. These include:

Nonlinearity - An artificial neuron can be linear or non-linear. If the network is made up of non-linear neurons, then it is a non-linear network. For solving problems in petroleum engineering, it is essential that the network is non-linear because the relationship between the input and output data is usually highly non-linear.

Input-output mapping - Neural networks learn the physics of a given system by constructing an input-output mapping of the problem at hand. No prior assumptions are made on a statistical model for the input data. Without this ability, no neural networks would be based on supervised learning.

Adaptivity - Neural networks need to be able to change their synaptic weights based on changes in the physical system. This implies a neural network trained to operate in a reservoir with 4 wells should be easily retrained to handle 5 wells. Also, a neural network can be designed to change its synaptic weights in real time when it is operating in a non-stationary environment. For example, in the limit, neural networks should be able to handle changes in reservoir conditions over time.

Contextual Information - Knowledge is represented by the structure and activation state of a neural network. It is assumed that contextual information is dealt with naturally by the neural network because of its inherent inter-connectivity. It would be a pertinent argument to state that neural networks cannot handle the complex physics of petroleum reservoirs. Also, a concern is how results from neural networks can be constrained to honor mass balance and geology of the reservoir. These are areas certainly worthy of further research.

Fault tolerance - Neural networks are capable of robust computation or are fault tolerant because their performance degrades gracefully under extreme operating conditions.

Uniformity of analysis and design - Most neural network architectures are basically information processors. Therefore, they all have neurons as their basic unit. This makes it possible to share theories and learning algorithms in different applications

of neural networks. Also, this implies modular networks can be built through a seamless integration of modules.

The three basic elements of a neuronal model are as follows:

- (a) A set of synapses each of which is represented by a weight of its own, w_{kj} , where k refers to the neuron and j refers to the synapse as shown in **Fig. 4.2**.
- (b) An adder for summing up the input signals.
- (c) An activation function for limiting the amplitude of the output of a neuron.

$$u_k = \sum_{j=1}^m w_{kj} x_j \quad (4.1)$$

$$y_k = \varphi(u_k + b_k) = \varphi(v_k) \quad (4.2)$$

$$\text{where } v_k = u_k + b_k \quad (4.3)$$

where $w_{k1}..w_{km}$ are synaptic weights of neuron k , $x_1...x_m$ is the input vector, u_k is the linear combiner output from the neuron, b_k is the bias and $\varphi(\bullet)$ is the activation function.

The model described above is a description of the basic unit of most networks including multi-layer networks.

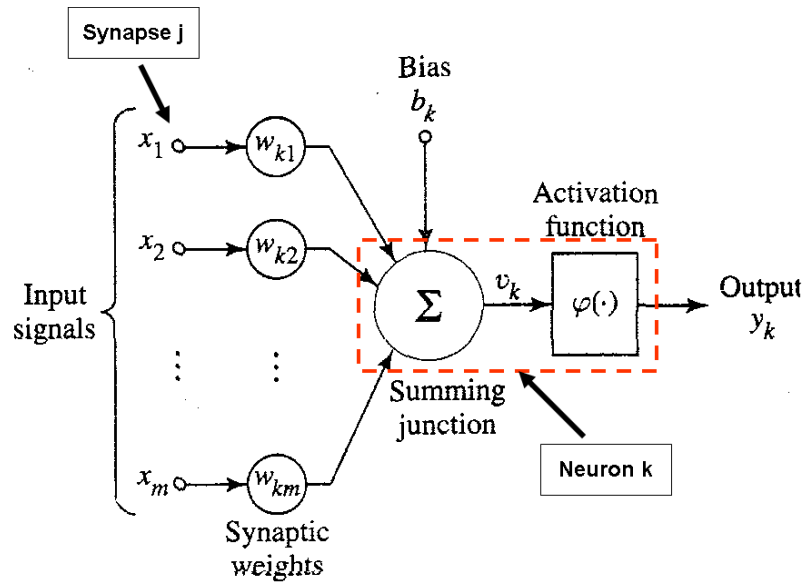


Figure 4.2- Representation of non-linear model of a neuron (modified from Haykin, 2005).

The activation function used for a given problem depends on the functional relationship between the input and output. It makes sense to conclude that to decipher relationships between non-linear variables, a non-linear activation function is required. For completeness, We mention that there are three basic types of activation functions. These include the (a) Threshold function (b) Piecewise –linear function and (c) Sigmoid function. The sigmoid function is more applicable to our problem because of its ability to model non-linear behavior. It is the most common activation function used in the construction of artificial neural networks. It can be defined in the two forms shown below:

$$\varphi_1(v) = \frac{1}{1 + \exp(-av)} \quad (4.4)$$

$$\varphi_2(v) = \tanh(v) \quad (4.5)$$

$\varphi_1(v)$ is the log-sigmoid function while $\varphi_2(v)$ is the hyperbolic tangent function. The shapes of the sigmoid and tangent function are as shown in **Fig. 4.3A and B**. A threshold function can only have value of 0 or 1 whereas a sigmoid function assumes a continuous range of values from 0 to 1. The sigmoid function is also differentiable. This is very important because the error back-propagation would not be possible if the function was not differentiable.

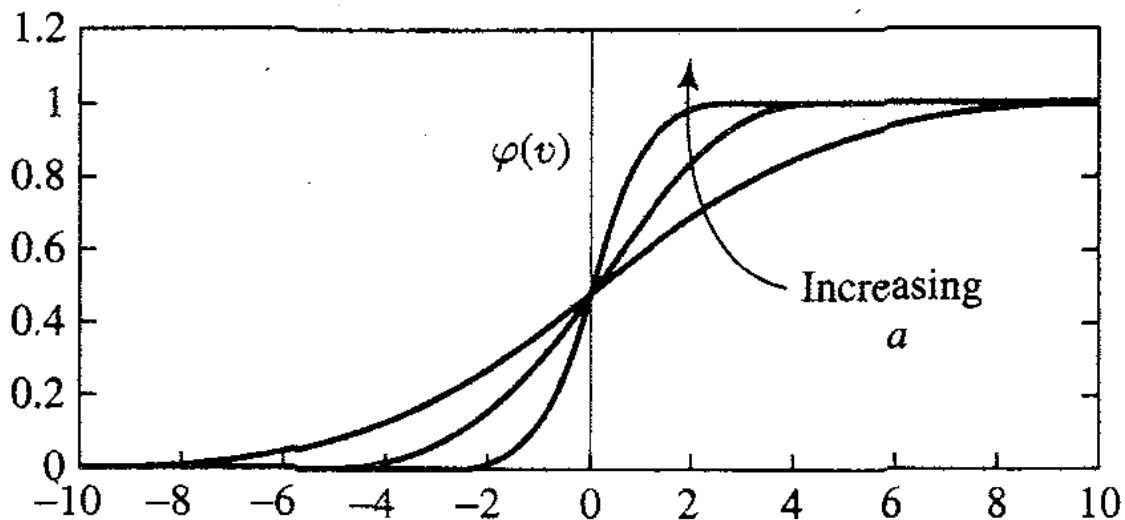


Figure 4.3A - Log-sigmoid function plot (Haykin, 2005).

The choice of neural network architecture is linked with the learning algorithm used to train the network. For the prediction of average water production from a well, we used multi-layered feed forward networks with error back propagation.

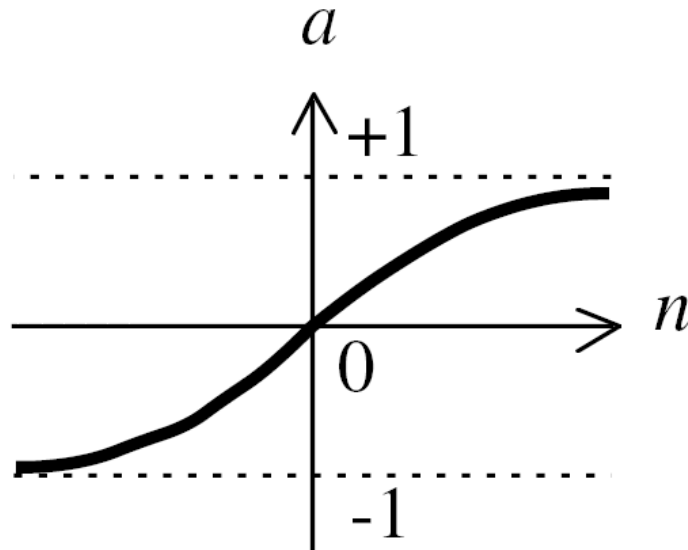


Figure 4.3B - Hyperbolic tangent function plot (Haykin, 2005).

There are three different classes of network architecture. They are:

- (a) Single Layer Feed forward Networks - This consists of an input layer of source nodes projected onto an output layer of neurons. The input layer is discounted because no computations occur there (**Fig. 4.4A**).
- (b) Multi-layer Feed forward networks - In this kind of network, there is at least one layer (called the hidden layer) between the input and output layers. The purpose of the hidden layer is to extract useful features from the input layer. It has been postulated that it would be possible to extract higher order statistics from the network because of the hidden layer (**Fig. 4.4B**).
- (c) Recurrent Neural Networks - The main difference between a feed forward network and a recurrent network is the presence of at least a feed-back loop from one of the neurons to itself or other neurons (**Fig. 4.4C**).

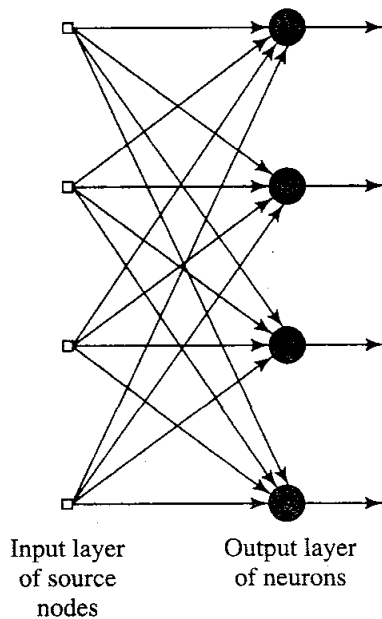


Figure 4.4A - Representation of a Single Layer Feed forward Network (Haykin, 2005).

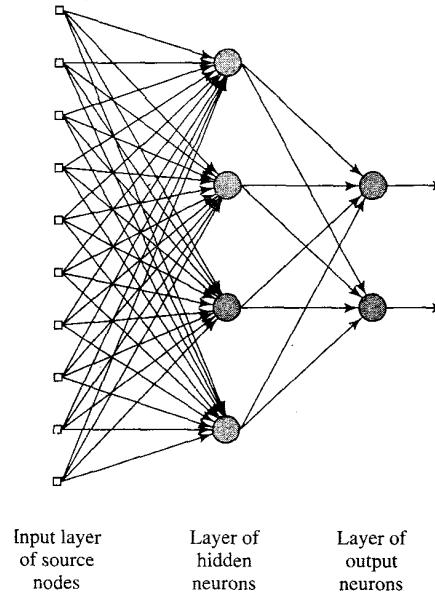


Figure 4.4B - Representation of a Multi-layer Feed forward network (Haykin, 2005).

Various learning rules are associated with these network architectures. The five basic learning rules include (a) Error-correction learning (b) Memory-based learning (c) Hebbian learning (d) Competitive learning (e) Boltzmann learning. Let us define the following terms (see Fig. 4.5); $\mathbf{x}(n)$ is the input vector (in our case, that would be the observations), n is the time-step of an iterative process involved in adjusting the synaptic weights of the neuron k . $y_k(n)$ is the output signal, $d_k(n)$ is the desired response, $e_k(n)$ is the error signal and $E(n)$ is the cost function.

For one neuron, we have the following:

$$e_k(n) = d_k(n) - y_k(n);$$

$$E(n) = 0.5 e_k^2(n) \quad (4.6)$$

The objective of error back-propagation is to minimize the cost function stated above using the delta rule (eqn. 4.6). The delta rule states that the adjustment made to a synaptic

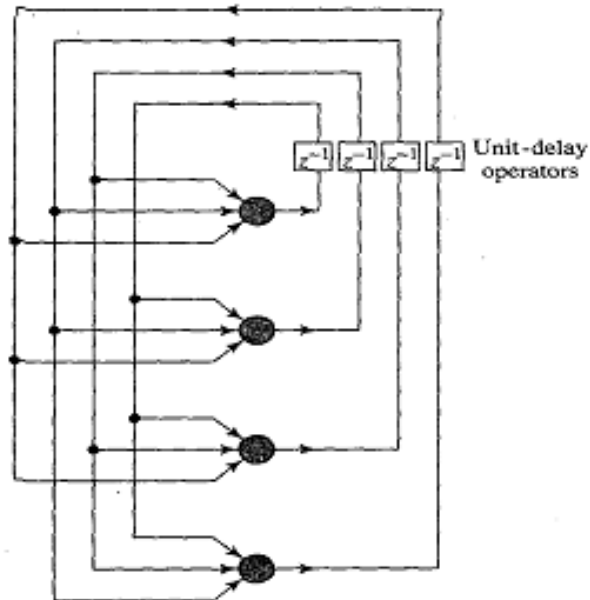


Figure 4.4C – Representation of a recurrent Neural Networks (Haykin, 2005).

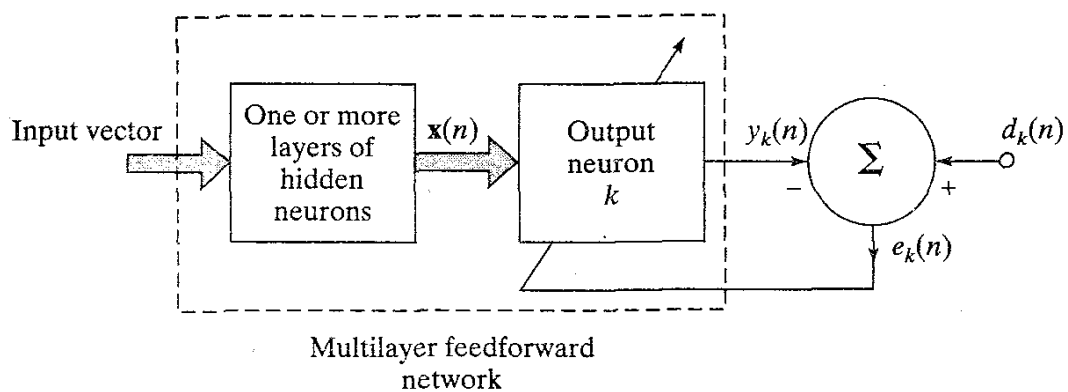


Figure 4.5- Block diagram of a neural network, highlighting the only neuron in the output layer (Haykin, 2005).

weight of a neuron is proportional to the product of the error signal and the input signal of the synapse in question. This rule can be modified for use in multi-layer networks. Error back propagation can be applied to single-layer feed-forward networks. It can also be applied to multi-layer feed forward networks with some modifications. Details of the mathematical derivation of these rules can be seen in Mitchell (1997) and Haykin (2005).

4.4 Determination of Training Set Size

The input and output of the neural network for average water prediction is as shown in **Fig. 4.1**. We already decided to use a feed- forward neural network with error back propagation. However, we still had to decide on the network topology (number of hidden layers) and the amount of training examples we required. We decided to start with a network with one hidden layer. This is because every bounded continuous function can be approximated with arbitrarily small error by a network with two layers, that is, networks with a sigmoidal hidden layer and unthresholded linear units at the output layer (Cybenko 1989; Hornik et al. 1989). We had no reason to assume the function between our input and output was not continuous. From the above, the only structure we varied in our network topology was the number of hidden units in the hidden layer. Next, we had to determine the minimum number of training examples required to train a two-layer neural network to a pre-determined accuracy. However, before we continue our discussion of this issue, we need to define the following terms; (1) Dichotomy (2) Shattering (3) Vapnik-Chevronenkis (VC) dimension. The term dichotomy refers to a binary classification function or decision rule (a function that can split a given training data set into two distinct parts), Haykin (2007). A set of instances, S is **shattered** by hypothesis space H if and only if for every dichotomy of S there exists some hypothesis

in H consistent with this dichotomy (Mitchell, 1997). This implies a given training set is shattered by a neural network (which has an infinite hypotheses space) if for every partition of the training set, there exists a neural network topology that can represent this partition. The VC dimension of a hypotheses space, $VC(H)$, defined over instance space X is the size of the largest finite subset of X shattered by H . This implies the VC dimension of a given neural network topology is the largest training dataset size that can be shattered or partitioned by the given neural network topology. Based on a review of neural network literature by Haykin (2005), we see that the VC dimension of a feed-forward neural network is of the order of W^2 , where W is the total number of free parameters in the neural network. W is determined by the number of weights and bias connections in the neural network. For example, the hypothetical network in **Fig. 4.4B** has 10 input nodes, 4 neurons in the hidden layer and 2 neurons in the output layer. Therefore it has a total of 48 neural connections and 6 bias connections. This implies $W=54$ for this system. If the VC dimension is of the order of W^2 , then the system has a VC dimension of ~ 2916 . Therefore, the more complex the networks, the higher the VC dimension. Also, from literature, we know that the number of training examples sufficient to learn with probability of at least $(1-\delta)$ any function to within error ϵ increases with increasing VC dimension, where δ and ϵ are small. Therefore for this work, let us assume that our initial network has 16 input nodes, 1 hidden layer containing 5 sigmoidal units and 1 output neuron. **Table 4.1** is a summary of the components of the network. It is reported by Haykin (2005) that there is a constant K such that a sufficient size of training set, N , for any algorithm is defined by **eqn. 4.7**

$$N = \frac{K}{\epsilon} \left[h \log \left(\frac{1}{\epsilon} \right) + \log \left(\frac{1}{\delta} \right) \right] \quad (4.7)$$

Fig. 4.6 shows the relationship between training set size and error parameter given constant values of K and δ using eqn. 4.7. The above analysis was done so that we could investigate the relationship between the parameters in **Fig. 4.6**. However, the results have limited practical significance. We assumed arbitrary values for K , ϵ and δ (confidence parameter).

Table 4.1– NEURAL NETWORK COMPONENT SUMMARY

Number of input nodes	16
Number of neurons in hidden layer	5
Number of neurons in output unit	1
Neural connections	80
Number of bias connections in hidden layer	5
Number of bias connections in output unit	1
Number of free parameters, W	91
VC dimension, $O(W^2)$	~ 8281
K	0.01
ϵ	0.05 – 0.5
δ	0.05

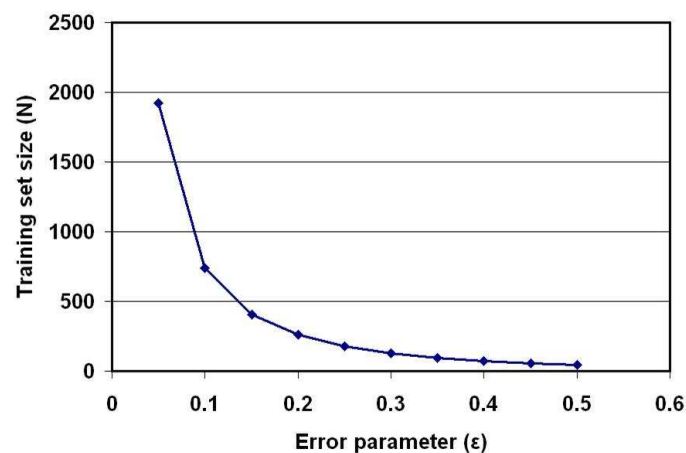


Figure 4.6- Dependence of training set size on error bounds.

This is because (1) We do not have a reliable estimate for K and (2) the theoretical analysis used to derive eqn. 4.7 assume worst case scenario, making the results to be pessimistic. Nonetheless, it is interesting to note the exponential drop in training set size requirement as the error bounds are relaxed. The number of training sets used to train the network was dependent mainly on time constraints and on our ability to collate the required data from several public databases. The wells from which the training dataset was compiled were selected randomly from the Denton and Parker Counties.

4.5 Determination of Hidden Structure in Data

Because of the multi-dimension nature of our dataset, it is impossible to determine the inner structure by visual inspection. Therefore, Hebbian and competitive learning based algorithms were considered in order to achieve this objective. We note that Hebbian learning algorithms are in general related to principal component analysis (PCA). The end point of principal component analysis is to determine eigenvalues and associated eigenvectors with a dimensionality less than that of the input vector. These eigenvalues represent the information content of the input dataset. For example, the straight line that fits the input-output mapping in **Fig. 4.7** is approximated by the eigenvector. However, we decided against using Hebbian learning based algorithms because as with PCA, these algorithms worked best when there is a linear relationship between input and output. We know that this is not likely to be the case for our dataset. We are aware that non-linear PCA techniques exist, but to the best of our knowledge, these algorithms have not been implemented generally in commercially available software like MATLAB. Therefore, as a matter of efficiency, we concentrated on the use

of competitive learning based algorithms, some of which are considered non-linear generalizations of principal components analysis. In competitive learning, the Euclidean distance between an input vector and the weight vector of a set of neurons is computed. The neuron whose weight matrix minimizes this distance wins and its weight connections are adjusted according to the learning rule in **eqn. 4.8**. The weight connection of all other neurons is unaffected.

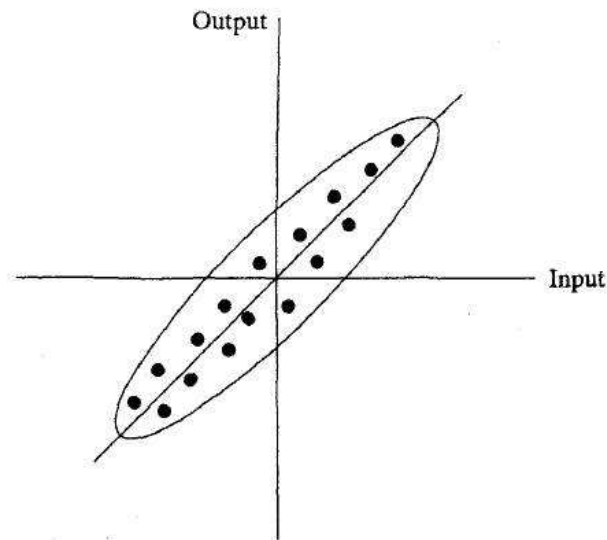


Figure 4.7– Two dimensional distribution produced by a linear input-output mapping (Haykin, 2005).

$$\Delta \bar{w}_{kj} = \begin{cases} \eta(\bar{x}_j - \bar{w}_{kj}) & \text{if neuron } k \text{ wins the competition} \\ \mathbf{0} & \text{if neuron } k \text{ loses the competition} \end{cases} \quad (4.8)$$

η is the learning rate parameter. ‘k’ refers to the kth neuron and ‘j’ refers to the size of the input vector. **Eqn. 4.8** has one constraint. The sum of all weights connecting a input vector to each neuron is unity. This constraint is expressed mathematically in **eqn. 4.9**.

$$\sum_j w_{kj} = 1 \quad (4.9)$$

The net effect of this learning rule is that input vectors with similar location in j -dimensional space will cluster around a specific neuron defined by its weights. Thus, ideally the number of neurons should equal the number of clusters in the data. It is important to note that the internal disarray within each cluster must be less in magnitude than the distance between different clustering for effective clustering. Therefore, the primary driver for clustering in competitive learning is competition between neurons, where the ‘winning’ neuron’s weight is adjusted according to a learning rule. One important method of internal organization based on competitive learning is a self-organized map (SOM). According to Haykin (2005), “A self organized map is characterized by the formation of a topographic (*surface configuration*) map of the input patterns in which *the spatial locations (i.e., coordinates) of the neurons in the lattice are indicative of the intrinsic statistical features contained in the input patterns...*”. The main process in competitive learning is competition between neurons. In a self-organized map, the main processes are (1) competition (2) co-operation and (3) synaptic adaptation. The process of competition between neurons has been described above. In self –organizing maps (*and in contrast to ‘pure’ competitive learning*), the connection weights of the winning neuron and some neighboring neurons are adjusted. The neighboring neurons whose weights are adjusted are determined according to a neighborhood function. The process by which the connection weights of the winning / neighboring neurons are adjusted is called synaptic adaptation. Synaptic adaptation in self-organized maps is based on the learning rule described in **eqn. 4.10**.

$$\Delta \bar{w}_j = \eta(n) h_{j,i(x)}(n) (\bar{x} - \bar{w}_j) \quad (4.10)$$

where $\Delta\bar{w}_j$ is the weight connection adjustment for every j th neuron in the self-organized map, $\eta(n)$ is the time dependent learning rate parameter, $h_{j,i(x)}(n)$ is the time dependent neighborhood function and $(\bar{x} - \bar{w}_j)$ is the misfit, in an Euclidean sense between the input vector and the weight vector of the j th neuron (see **Fig. 4.8**). Our ability to successfully use a SOM to identify the underlying structure in the dataset would depend on our choice of the learning rate parameter and the neighborhood function.

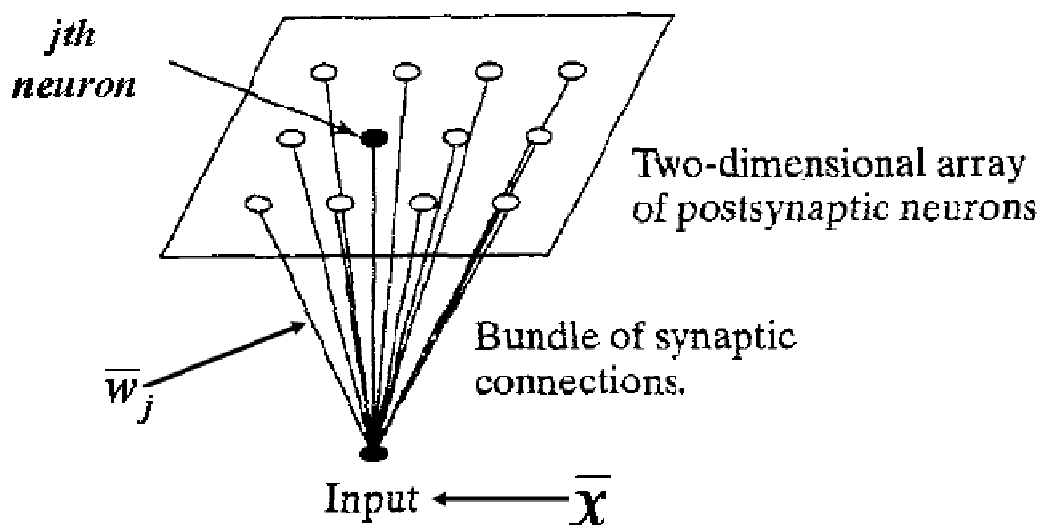


Figure 4.8– Kohonen model of a self-organized map (modified from Haykin, 2005).

Denton County has about 2500 wells drilled to access the Barnett Shale. We randomly sampled about 450 wells (containing deviated, vertical and horizontal wells) from this population. Each well was represented by a input vector containing about 18 parameters – see **Table 4.2**. In order to determine the structure in this dataset (if any), we

used a self organizing map to analyze the data. We used a 10-by-10 array of 100 neurons with rectangular grid-block typology. **Fig. 4.9** shows the topology of the self-organized map. This network was implemented in MATLAB. After 100 iterations, we can observe in **Fig. 4.10** that the data has been clustered into at least two groups.

Table 4.2– PARAMETERS IN INPUT VECTOR FOR DENTON AND PARKER COUNTIES

<u>Input</u>	<u>Description</u>
1	Rank
2	Perforation Interval (feet)
3	Fracturing fluid Volume (barrels)
4	Proppant quantity (pounds mass)
5	Number of fracture stages
6	Tubing depth (feet)
7	Casing depth (feet)
8	Flowing Tubing Pressure –FTP (pounds per square inch)
9	Choke size (1/64")
10	Shut in Tubing Head Pressure – SITHP (pounds per square inch)
11	Specific gravity of gas (dimensionless)
12	Well Type (deviated = '1', horizontal = '2', vertical = '3')
13	Latitude
14	Longitude
15	Gas Production per month (Million standard cubic feet / month)
16	Number of months completion produced
17	Acid pumped or not (Acid not pumped = '1', Acid pumped = '2')
18	Water production per month (Barrels / month)

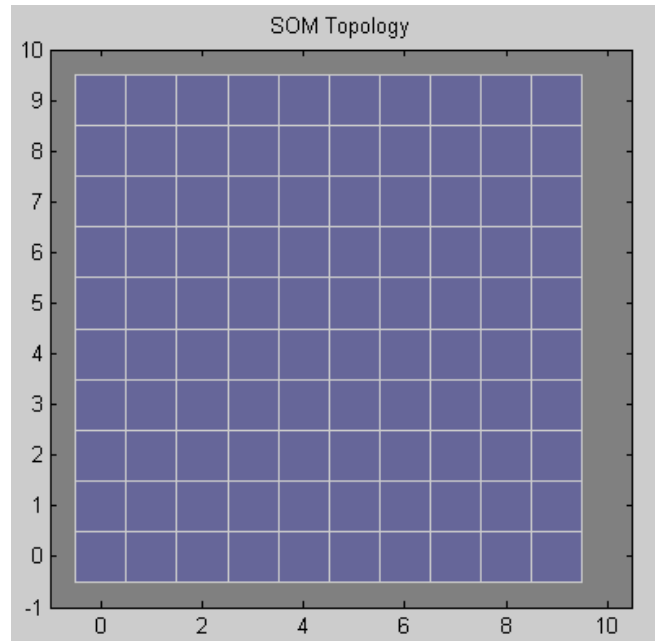


Figure 4.9– 2D SOM topology using 10x10 neurons with rectangular grid block typology.

In order to interpret **Fig. 4.10**, it is important to note the following as explained in the MATLAB technical documentation:

- (a) The blue rectangles represent the neurons.
- (b) The red lines connect neighboring neurons.
- (c) The colors in the regions containing the red lines indicate the distances between the neurons. The darker colors represent larger distances while the lighter colors represent smaller distances. We note that there is a gradual lightening in color from the lower triangular section of **Fig. 4.10** to the upper triangular section of the same figure. There is some internal scatter even in the clustered portions of the dataset as seen in the darker parts of the upper triangular section and the lighter parts of the upper triangular section. This result suggests the dataset can be clustered into at least two subsets. The physical properties of these clusters is however unknown.

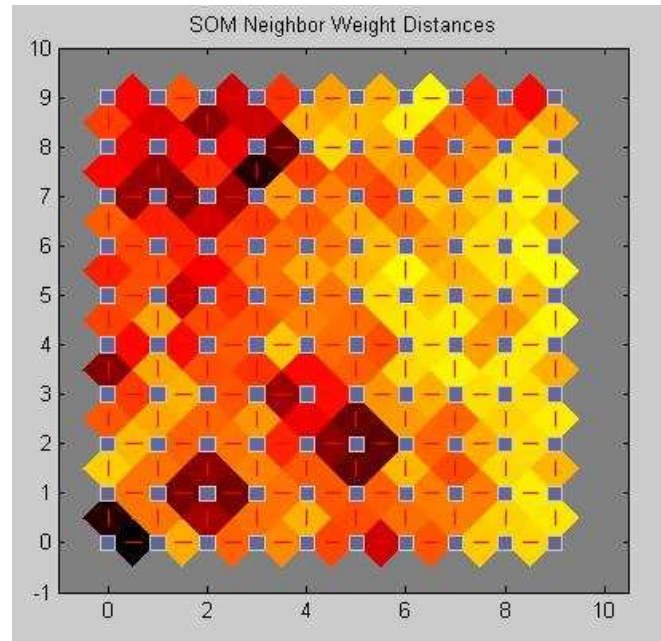


Figure 4.10 – Color-coded representation of self organized map neighbor weight distances for deviated, horizontal and vertical wells, number of iterations = 100.

In order to investigate the physical basis on which the SOM clusters this dataset, we tried the following. Using the input vectors from 20 high water producing wells; a SOM produced the results seen in **Fig. 4.12 & 4.13**. If **Fig. 4.12** was examined in isolation, it would seem that the map classified the data into 2 main regions. However, a plot of the SOM layer showing the number of input vectors classified by each neuron in the map shows otherwise (**Fig. 4.13**). The presence of the distinct boundary in **Fig. 4.12** is because the neurons in the upper right triangular part of the map did not ‘capture’ any input vectors.

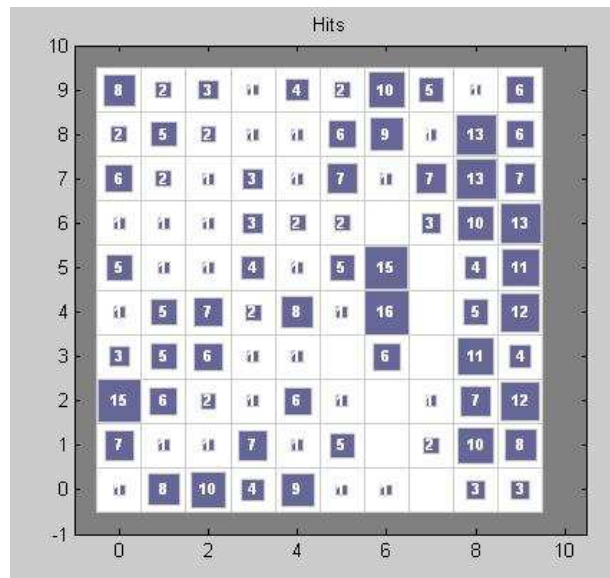


Figure 4.11 – 2D SOM layer for all wells with each neuron showing the number of input vectors that it classifies, number of iterations = 100, number of examples = 450.

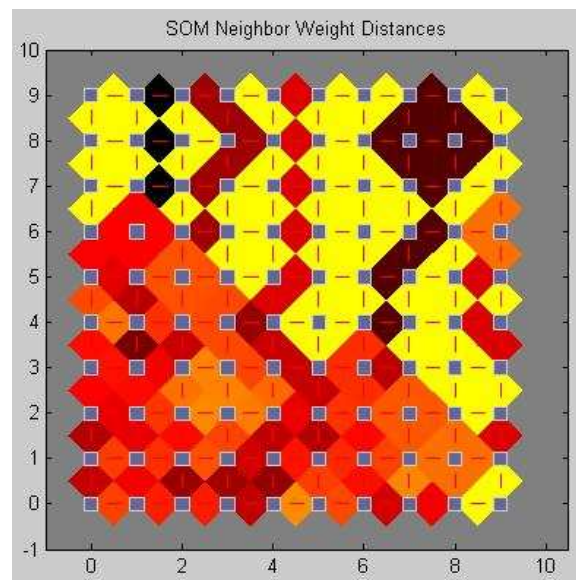


Figure 4.12 – Color-coded representation of self organized map neighbor weight distances for 20 high water producers, number of iterations = 100.

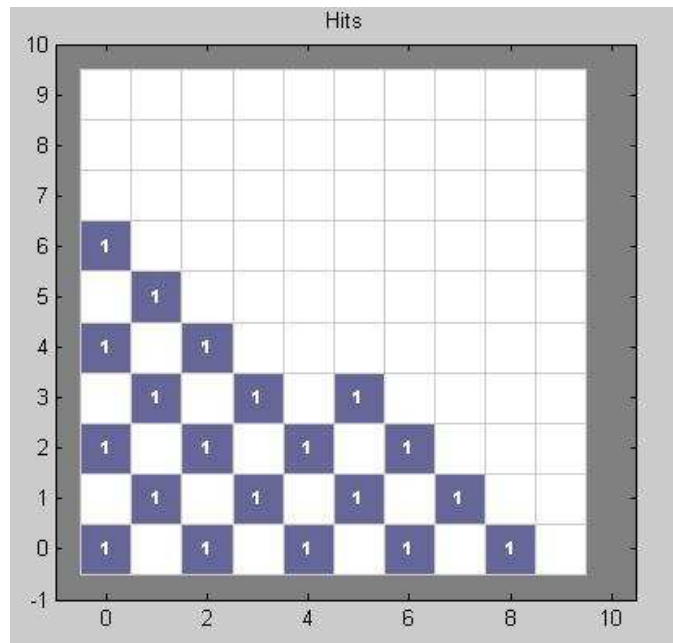


Figure 4.13 – 2D SOM layer for wells with high water production with each neuron showing the number of input vectors that it classifies, number of iterations = 100, number of examples = 20.

Based on **Figs. 4.10, 4.11, 4.12 & 4.13**, we can hypothesize that the high water producing wells are clustered in the lower left triangular part of **Fig. 4.10** while the low water producing wells are clustered in the upper right triangular part of the same figure.

In summary, we have used the SOM to do the following:

- a) Identify the fact that the dataset is divided into 2 main clusters. Cluster 1 is defined by the darker colored sections in **Fig. 4.10** and Cluster 2 by the lighter colored sections in **Fig. 4.10**.
- b) It is our hypothesis based on the comparison of **Figs. 4.10, 4.11, 4.12 and 4.13** that the dark colored sections in **Fig. 4.10** depict neurons representing the high water producers in the dataset while the light colored sections depict neurons representing the low water producers.

Another way to visualize the data is to use the k-means algorithm. This objective of this algorithm is to define partition(s) such that data points in each cluster are as close together as possible and are far away from data points in other clusters as possible. We used the implementation of this algorithm in MATLAB to investigate the structure in our dataset. In order to visualize the degree of separation between the resulting clusters, we used the Silhouette plot. This plot displays a measure of how close data points in different clusters are. This measure ranges from +1 to -1. A value close to 1 indicates data points that are very distinct from neighboring clusters, silhouette values close to zero indicate data point can be easily mis-classified while values less than zero indicate data points that may have been assigned to the wrong cluster. As input in the k-means algorithm in MATLAB, we need a guess as to the number of clusters we expect in the data set. The optimum number of clusters is one that maximizes separation between individual clusters. Well defined clusters are expected to have higher average silhouette values when compared to less defined clusters. **Fig. 4.14** shows the Silhouette plot for our dataset. We analyzed our data with the k-means algorithm assuming 2, 3 and 4 clusters. **Table 4.3** shows the mean silhouette value for each run. We see that the average silhouette value is maximized when the number of clusters is equal to 2.

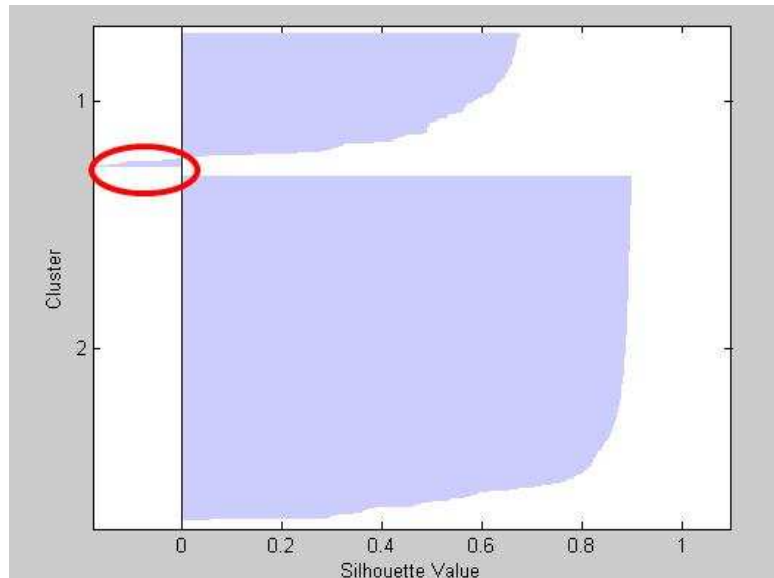


Figure 4.14– Silhouette plot for data set.

We therefore conclude that the data set under consideration can be partitioned into at least 2 clusters. There is also some potential for mis-classification as seen the region specified by the red oval circle in **Fig. 4.14**.

Table 4.3 – AVERAGE SILHOUETTE VALUES FOR INCREASING NUMBER OF CLUSTERS

<u>Number of Clusters</u>	<u>Average Silhouette value</u>
2	0.7462
3	0.6711
4	0.5106

4.6 Determination of Whether A Well Drilled in Denton County of the Barnett Shale Will Produce water

The first question we would try to provide an answer to is whether we can determine the water production potential of a new well given the data input specified by **Table 4.2**. Actually, the question is binary in nature and it goes as follows; will a new well produce water or not? This implies the wells in the data set that we have acquired must be classified into two classes namely, (1) class of water producers (2) class of non-water producers. We can attempt to answer these questions using (1) supervised (feed-forward neural network architecture, (2) unsupervised networks based on competitive learning and (3) supervised version of networks based on competitive learning called vector quantization networks. We analyzed the dataset from Denton County using feed forward neural network architecture. **Fig. 4.15** shows the input and output of the neural network. The input vector to the neural network is the RHS of Fig. 4.15 while the expected output is on the LHS. The neural network was a 2-layer network and the number of neurons in the hidden node was varied between 5 and 20. Increasing the number of neurons reduced training sample misfit as expected. However, with this increase, the general neural network performance degraded on the application of the testing dataset. The results were inconclusive and are shown in **Fig. 4.16**. We note that if the neural network outputs a number equal or close to '1', the well is deemed as a potential water producer and if the neural network outputs equal or close to '2', the well is deemed as a potential non-water producer. We also note that the output from this network can be potentially any real number. Therefore, based on the fore-going, one of the

challenges we faced was to define a threshold based upon which we could decide when a well was likely to be a water producer and vice versa.

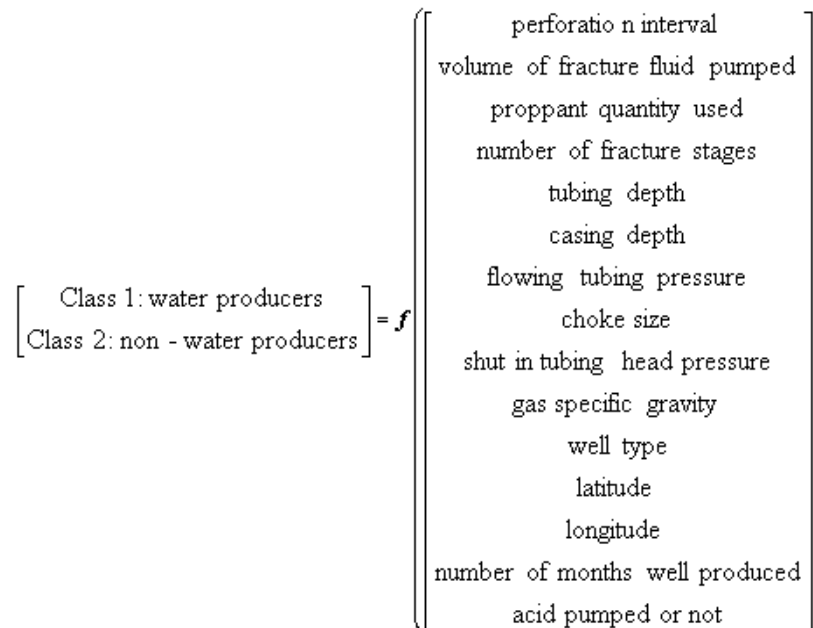


Figure 4.15– Output and input of feed-forward neural network for water production potential classification.

For example, as shown by the dotted horizontal line in **Fig. 4.16**, if we chose our threshold to be 1.4, the network would misclassify a lot of water producers as non-water producers and vice versa. The red oval shapes in **Fig. 4.16** are the misclassified data points based on our arbitrary threshold of 1.4. Also, computing the misclassification potential of this network could be cumbersome to implement (because it is dependent on the definition of an arbitrary threshold value). As a result of these complications, we decided to try out our second option, that is, the use of unsupervised networks based on competitive learning. We undertook a brief description of competitive learning in Section 4.5. Here, we apply this algorithm to our dataset. The input vector into the competitive

neural network is as shown in **Fig. 4.15**. In order to ensure certain elements in the input vector are not weighted heavily compared to other elements, we ensured the values of the elements of the input vector were normalized to between 0 and 1. This was done by dividing the parameters by their maximum value. The number of neurons used in competitive networks is dependent on the number of classes the dataset is classified into. In our case, the number of classes was 2 (see LHS of **Fig. 4.15**). We used cross-validation to ensure our estimate of misclassification error was representative of the dataset. Cross-validation is a process by which a network is trained repeatedly using different versions of the same dataset. The different versions are generated by randomizing the dataset using a random number generator. The end result is an error estimate that is averaged over a series of runs; in this case, we made 10 runs.

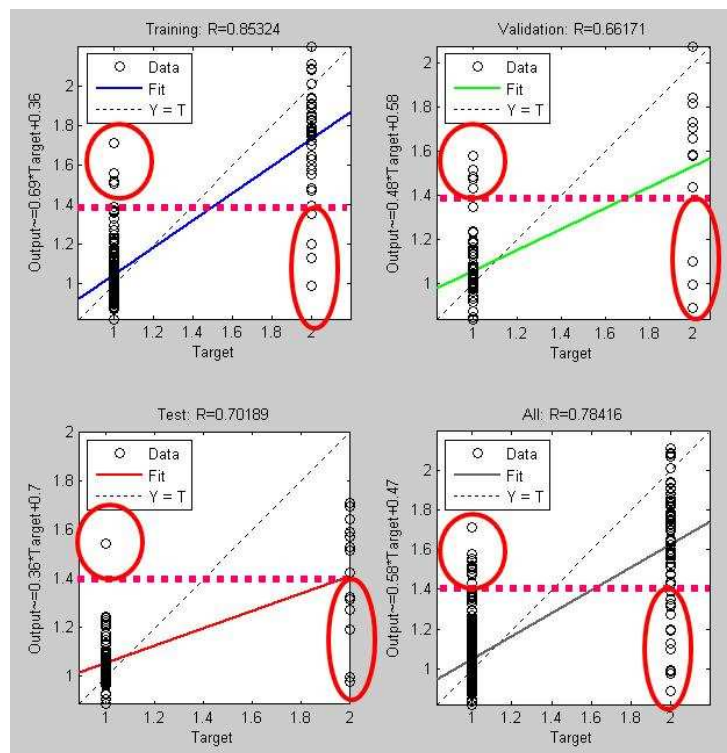


Figure 4.16– Results of feed-forward neural network for classification purposes.

Table 4.4 summarizes the results from these runs. We can see that the misclassification error estimate is very high (it can be interpreted to mean that we have a 50:50 chance of misclassifying a water producer as a non-water producer and vice versa). This result is surely not good enough. The input vector in the RHS of **Fig. 4.15** does not contain any indication that we have prior knowledge about the water production potential of a well.

Table 4.4– SUMMARY OF RESULTS FOR COMPETITIVE NEURAL NETWORK

	<u>Average misclassification error</u>	<u>Misclassification error standard deviation</u>
Vertical Wells	0.4934	0.0292
Horizontal Wells	0.5152	0.0483
All Wells (vertical, deviated and horizontal)	0.4830	0.0262

Based on the above results, we can intuitively state that we can improve our results by incorporating our prior knowledge of water production potential of a well into our algorithm. This reasoning led us to consider the use of our third option; vector quantization, which is a supervised form of competitive learning. **Fig. 4.17** is a block diagram that describes the vector quantization algorithm.

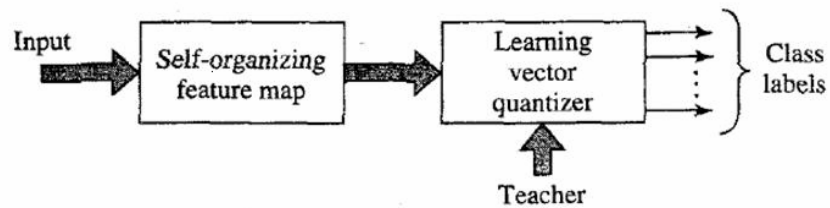


Figure 4.17- Block diagram of adaptive pattern classification, using a SOM and a learning vector quantizer (Haykin, 2005).

The input in **Fig. 4.17** is the RHS of **Fig. 4.15**. The basic competitive network acts as a self-organized map. It classifies the dataset into different sets; each set is called a Voronoi cell. Each Voronoi cell has a center called the Voronoi vector. The ‘teacher’ is a vector that contains a representation of our prior knowledge regarding the system. The learning vector quantizer compares the class assignment of the SOM to that of the teacher. If they match, the Voronoi vector is moved in the direction of the input vector. If they do not match, the Voronoi vector is moved away from the input vector. At the end of training, the misclassification error of the algorithm is minimized. We also used the cross-validation technique to obtain a reliable estimate of classification error. We trained the quantizer with 80% of the dataset and validated the results with 20% of the dataset. **Table 4.5** summarizes the results of these runs.

Table 4.5– SUMMARY OF RESULTS FOR VECTOR QUANTIZER

	<u>Average misclassification error</u>	<u>Misclassification error standard deviation</u>
Vertical - 273 Wells	0.1036	0.0193
Horizontal – 125 Wells	0.4160	0.0280
All – 446 Wells (deviated, vertical and horizontal)	0.0910	0.0036

We can see that our results are much better and that we can reliably predict if a well would produce water or not based on the input data represented by the RHS of **Fig. 4.15**. The misclassification error for horizontal wells is higher compared to that of a vertical well. We observe that the mis-classification error increases with increasing

proportion of non-water producers in the data-set. We will suggest a reason for this trend in the next section.

4.7 Prediction of Average Water Production for A New Well Drilled in the Denton and Parker Counties of the Barnett Shale

In this section, we develop a neural network that will predict a value for average water production from a new well in Denton County. For previous analysis, we have used an input vector containing 18 parameters (see **Table 4.2**). The first input in **Table 4.2** is called the ‘rank’. For each category of wells, that is, vertical or horizontal, the wells located in Denton / Parker Counties were sorted in the order of decreasing water production. Consequently, each well was assigned a particular rank; from 1 to n based on its average water production data; where n is size of the dataset. The other parameters in the input vector are self-explanatory and are collated from government and public databases. Preliminary runs were made using a 2-layer neural network with 5 hidden neurons. A dataset consisting of vertical wells from Denton County was used. Using the mean prediction error (average over 100 network runs; error distribution was exponential) between the network output and the target water production values as the performance measure, we found out the following for both vertical and horizontal wells:

- (1) The ‘rank’ is an important variable for the prediction of average water production (compare **Figs. 4.18 and 4.19; Table 4.6**).
- (2) Better network performance is obtained if the output is the natural logarithm of water production as opposed to ‘raw’ water production data (compare **Figs. 4.18 and 4.20; Table 4.6**). Using the logarithm of the

average water production also increases the consistency of the network performance.

The rank is not a variable the engineer would have for a new well. Whether the rank can be predicted using available data is a question that would be answered in a later part of this section. However at first, we decided to train a neural network using data from both Denton and Parker Counties (inputs 1-7, 8, 11, 13-14, 17 of **Table 4.2**) with the aim of predicting water production (row 18). Some parameters in the input vector were omitted because the engineer might not have a reasonable estimate of their value. Different networks were trained for vertical and horizontal wells in both counties. We used the Levenberg-Marquardt algorithm implementation in MATLAB in order to minimize the error function. **Table 4.7** and **Fig. 4.21-4.24** summarizes results from these runs.

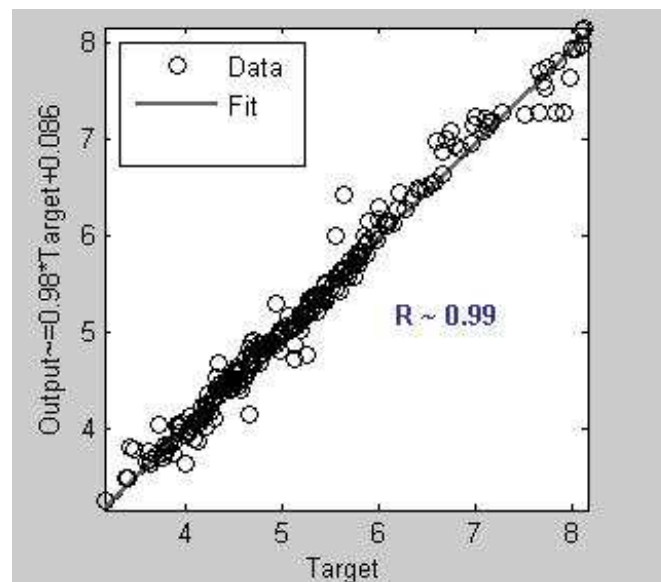


Figure 4.18– Influence of ‘rank’ on neural network performance; performance on training, testing and validation datasets (rank in input vector, target is logarithm of water production).

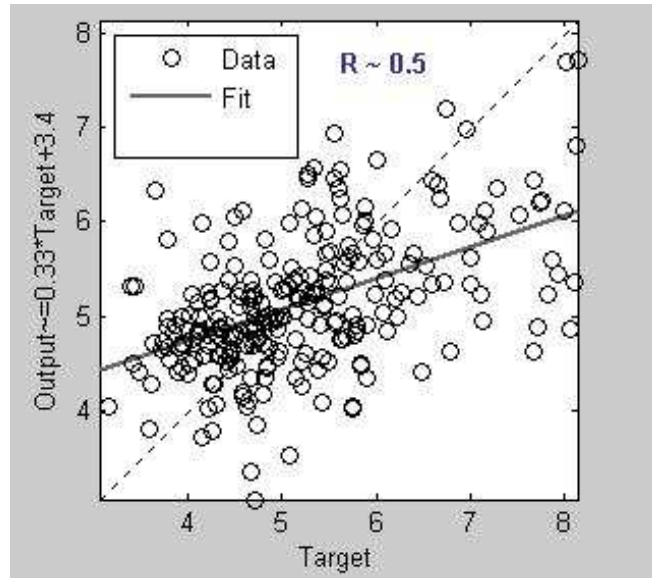


Figure 4.19– Neural network performance, rank not in input vector (target is logarithm of water production).

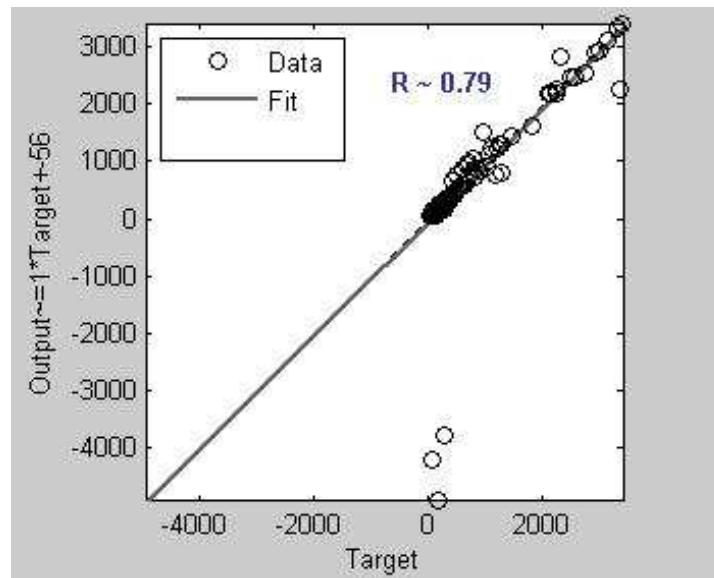


Figure 4.20– Neural network performance (rank in input vector, target is 'raw' water production).

Table 4.6– INFLUENCE OF RANK ON NETWORK PERFORMANCE

	<u>Average Prediction Error</u>	<u>95% confidence interval</u>
Rank in input vector, logarithm of water production as output	0.1443	[0.1279;0.1639]
Rank not in input vector, logarithm of water production as output	1.1993	[1.0635;1.3630]
Rank in input vector, raw water production data as output	0.6985	[0.6194;0.7938]

Therefore, we see that in order to be able to predict water production potential of a well, we need to have a good idea of its rank. A way of predicting the rank for a new well would be to find an input vector in the dataset that is closest in distance to the input vector for the new well. The rank of the input vector in the dataset can be used as the ‘expected value’ of the rank for the new well. However, we noted that a limitation of this approach is that the results we get might not be unique. This is because the input vectors in our dataset are quite similar (based on their dot product). We also think that the similarity between the input vectors is the reason why it is difficult for the neural network to predict average water production to a reasonable degree of accuracy without introducing the rank.

Table 4.7 - SUMMARY OF NEURAL NETWORK RESULT RUNS

<u>County</u>	<u>Well Type</u>	<u>Number of neurons in hidden layer</u>	<u>Average Prediction error over 100 runs</u>	<u>95% confidence interval</u>
Denton, dataset size = 250	Vertical	2	0.1768	[0.1568,0.2010]
		5	0.1183	[0.1049,0.1344]
		10	0.1098	[0.0974,0.1248]
		15	0.1117	[0.0991,0.1270]
		20	0.1154	[0.1023,0.1311]
Denton, dataset size = 62	Horizontal	2	0.4461	[0.3530,0.5819]
		5	0.3008	[0.2380,0.3923]
		10	0.2628	[0.2080,0.3428]
		15	0.2787	[0.2205,0.2787]
		20	0.3308	[0.2617,0.4314]
Parker, dataset size = 58	Vertical	2	0.3387	[0.2660,0.4460]
		10	0.2595	[0.2038,0.3418]
		15	0.2309	[.1813,0.3040]
		20	0.2933	[0.2303,0.3862]
Parker, dataset size = 219	Horizontal	2	0.2091	[0.1840,0.2398]
		5	0.1947	[0.1713,0.2233]
		15	0.2111	[0.1856,0.2420]
		20	0.2085	[0.1835,0.2392]

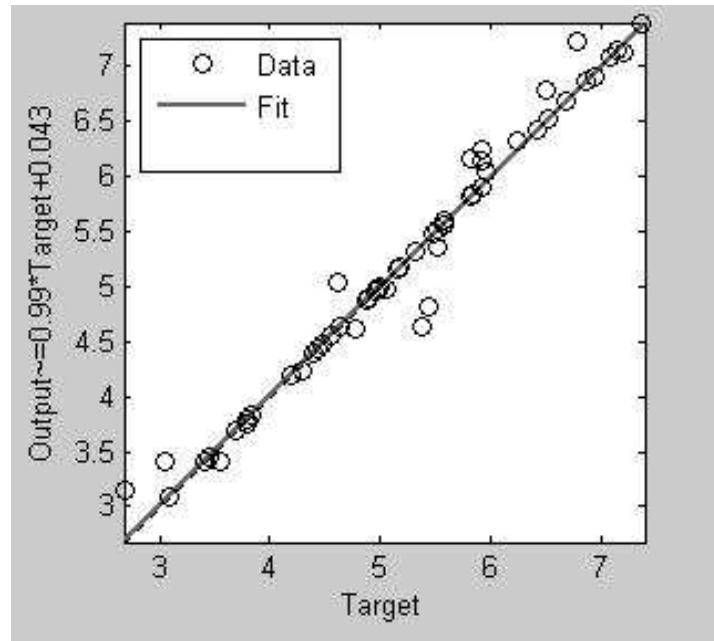


Figure 4.21– Network output versus target for vertical wells in Parker County, rank included. Dataset size =58 (number of hidden layers =1; number of neurons in hidden layer =8).

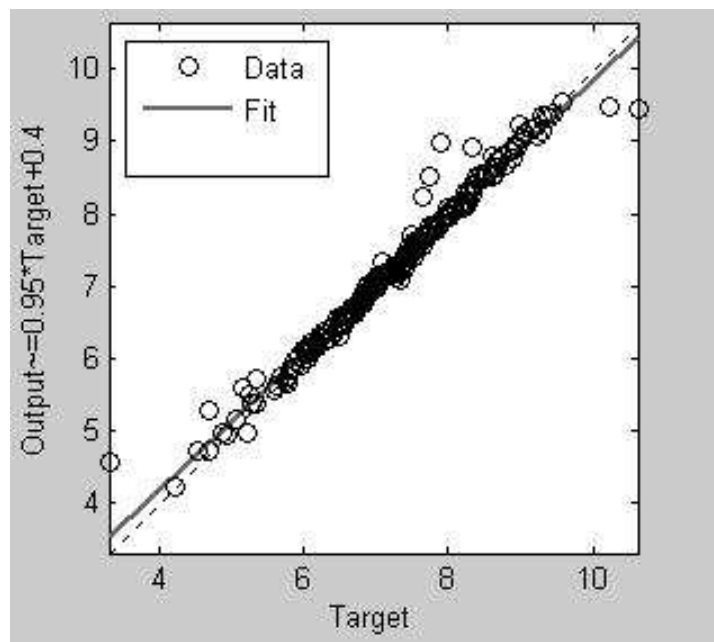


Figure 4.22– Network output versus target for horizontal wells in Parker County, rank included. Dataset size =219 (number of hidden layers =1; number of neurons in hidden layer =5).

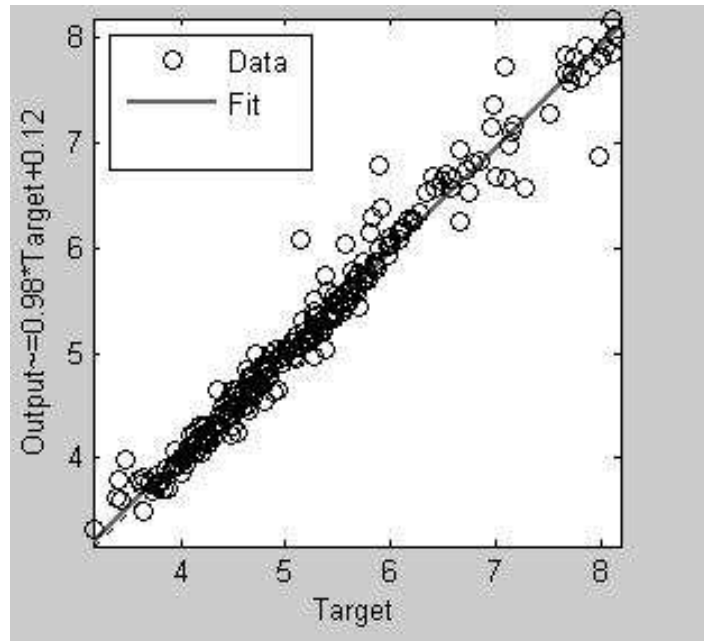


Figure 4.23 – Network output versus target for vertical wells in Denton County, rank included. Dataset size =250 (number of hidden layers =1; number of neurons in hidden layer =10).

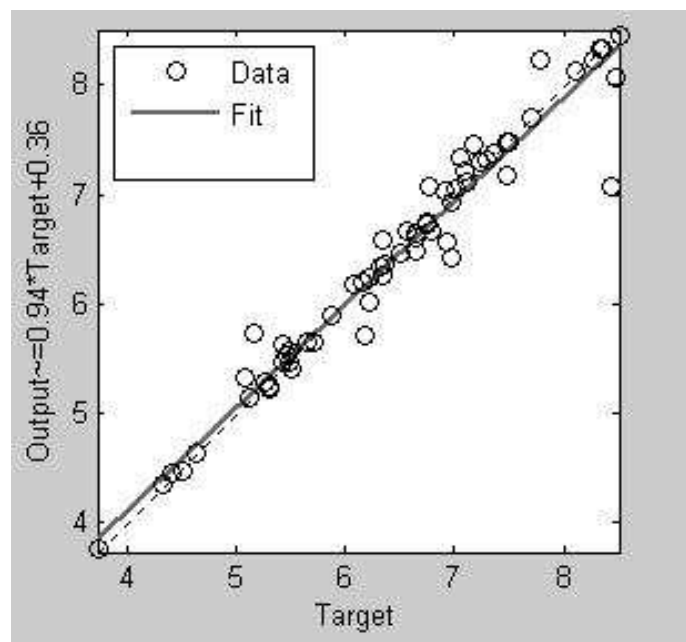


Figure 4.24– Network output versus target for horizontal wells in Denton County, rank included. Dataset size =219 (number of hidden layers =1; number of neurons in hidden layer =5).


4.8 Prediction of Well Rank Using Parameters Contained in Neural Network Input

Vector

In the previous section, we predicted the water production potential of wells drilled in both Denton and Parker Counties. A requirement of the input vector required to train the neural network was the rank. As previously stated the engineer would not have a value for the rank. We describe in this section, a procedure for determining the rank for a new well using the training dataset. To illustrate this point, we will use the training data set we compiled for horizontal wells in the Parker County.

Let us assume we want to predict the rank of one of the wells in the training dataset. The first step would be to compute the dot product between the normalized version of the input vector represented by this well and all the other input vectors in the dataset. This is to ascertain their similarity; the assumption being that similar input vectors would have similar rank. For example, in **Fig. 4.25**, Column 1 is the dot product of the input vector of well 1 and 218 other wells in the data set. Based on the results specified in Fig. 4.25, the engineer would make a determination as to the vectors that are closest to the new well vector. This is analogous to the definition of a neighborhood function in unsupervised learning. Using the rank associated with the chosen vectors, we define P10, P50 and P90 values of rank for the new well. These values define the low, medium and high rank predictions for the new well. The values for rank can be used as input part of the input vector into a neural network in order to predict P10, P50 and P90 values for average water production. Repeating this process for all the wells in our training set yields **Fig. 4.26**. Fig. 4.26 is a plot of P10, P50 and P90 values for water production for the 219 wells in our training database from Parker County.

Column 1



	1	2	3	4	5	6	7	8	9	10
196	0.9992	0.9993	0.9992	0.9991	0.9988	0.9991	0.9985	0.9990	0.9990	0.9981
197	0.9992	0.9992	0.9991	0.9991	0.9988	0.9991	0.9985	0.9990	0.9989	0.9981
198	0.9986	0.9989	0.9990	0.9991	0.9988	0.9990	0.9985	0.9988	0.9989	0.9980
199	0.9986	0.9989	0.9990	0.9990	0.9987	0.9990	0.9983	0.9986	0.9987	0.9980
200	0.9986	0.9983	0.9982	0.9980	0.9975	0.9979	0.9971	0.9986	0.9986	0.9980
201	0.9985	0.9982	0.9981	0.9979	0.9975	0.9977	0.9970	0.9985	0.9986	0.9979
202	0.9984	0.9981	0.9980	0.9978	0.9973	0.9977	0.9968	0.9984	0.9985	0.9979
203	0.9983	0.9980	0.9978	0.9977	0.9971	0.9976	0.9966	0.9984	0.9983	0.9979
204	0.9982	0.9978	0.9977	0.9975	0.9970	0.9974	0.9965	0.9984	0.9983	0.9979
205	0.9981	0.9977	0.9976	0.9974	0.9968	0.9973	0.9963	0.9983	0.9983	0.9979
206	0.9975	0.9971	0.9969	0.9967	0.9961	0.9966	0.9955	0.9977	0.9978	0.9976
207	0.9974	0.9970	0.9968	0.9966	0.9959	0.9965	0.9954	0.9976	0.9977	0.9975
208	0.9962	0.9957	0.9955	0.9953	0.9945	0.9951	0.9939	0.9965	0.9965	0.9969
209	0.9953	0.9948	0.9946	0.9943	0.9935	0.9942	0.9928	0.9957	0.9958	0.9968
210	0.9944	0.9938	0.9936	0.9933	0.9923	0.9931	0.9916	0.9948	0.9949	0.9967
211	0.9922	0.9915	0.9912	0.9909	0.9898	0.9907	0.9889	0.9926	0.9928	0.9950
212	0.9902	0.9894	0.9891	0.9887	0.9875	0.9885	0.9866	0.9907	0.9909	0.9934
213	0.9866	0.9857	0.9853	0.9849	0.9835	0.9847	0.9824	0.9872	0.9874	0.9904
214	0.5564	0.5522	0.5506	0.5486	0.5420	0.5479	0.5371	0.5599	0.5612	0.5769
215	0.5451	0.5409	0.5393	0.5372	0.5306	0.5366	0.5256	0.5486	0.5500	0.5658
216	0.5411	0.5369	0.5352	0.5332	0.5265	0.5326	0.5216	0.5446	0.5460	0.5618
217	0.5274	0.5231	0.5215	0.5194	0.5126	0.5187	0.5076	0.5309	0.5323	0.5484
218	0.3253	0.3206	0.3187	0.3164	0.3089	0.3157	0.3034	0.3293	0.3308	0.3487
219	0.1411	0.1362	0.1342	0.1318	0.1240	0.1311	0.1182	0.1453	0.1468	0.1657

Figure 4.25– Dot product of normalized input vectors in training dataset.

The reasoning applied to water production data in Sections 4.7 & 4.8 can be extended to gas production data. **Fig. 4.27** is a plot of P10, P50 and P90 values for gas production for the 215 wells in our training database from Parker County.

We note that the prediction made by the neural network is very much dependent on the quality or otherwise of the data. In Section 3, we made mention of the possibility that some of the data might be allocated. If this is the case, the predictions from this model would not be correct. However, the methodology used to solve the problem at hand would still be applicable once quality data can be accessed.

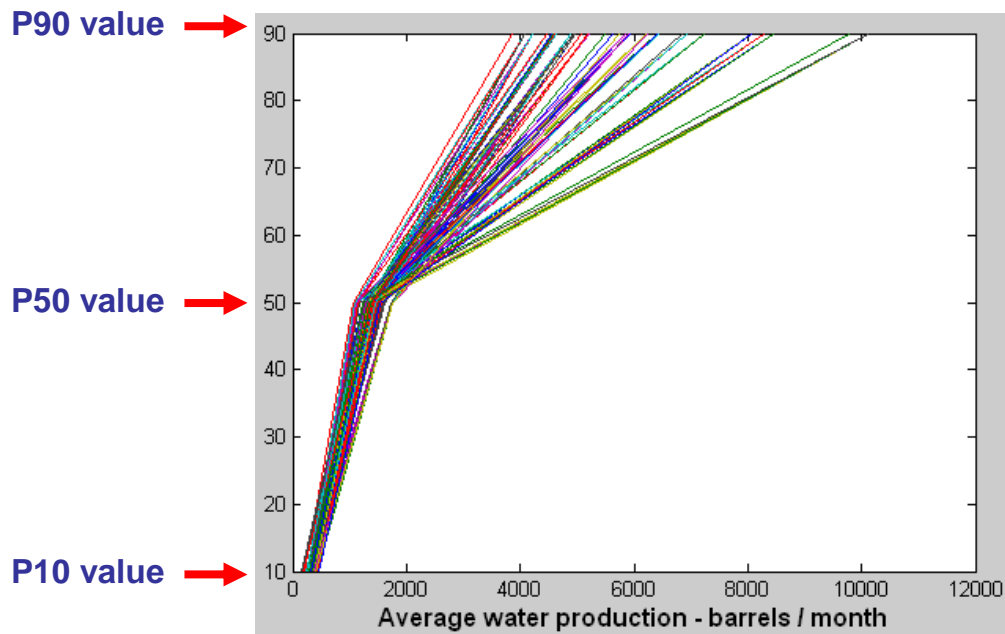


Figure 4.26 – P10, P50 and P90 predictions of water production for horizontal wells drilled in the Parker County of the Barnett Shale.

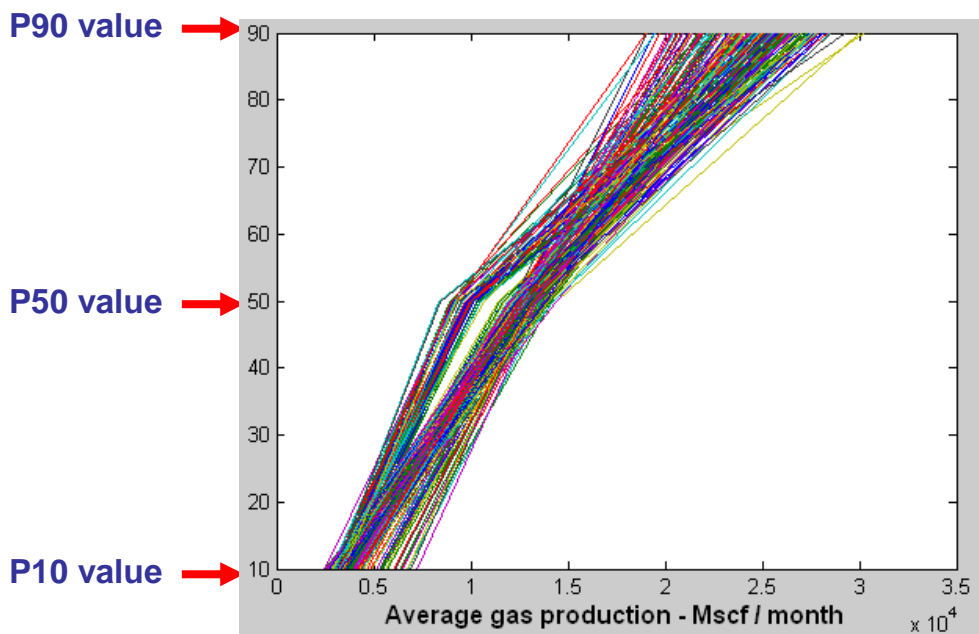


Figure 4.27 – P10, P50 and P90 predictions of gas production for horizontal wells drilled in the Parker County of the Barnett Shale.

4.9 Section Summary

We achieved the following in this section:

- Reviewed general machine learning and neural network theory.
- Investigated the structure of data from the Denton County of the Barnett shale and developed learning algorithms to predict water production potential from a new well drilled in the Denton or Parker County of the Barnett Shale.

5 CONCLUSIONS AND RECOMMENDATIONS

5.1 Conclusions

Based on a statistical analysis of production data from the Barnett Shale, we found that wells in the Core Area of the Barnett Shale are better producers. Also, for wells with the same completion type (vertical, deviated or horizontal), location is more important than time of completion or hydraulic fracturing strategy.

On the average, wells in the non-core area produce less water. The average vertical well in Denton and Parker Counties of the Barnett Shale currently experience liquid loading. Because the Turner equations do not take into consideration well deviation, it is likely that the average horizontal well in Parker County or even Denton County is also susceptible to liquid loading.

Based on analysis of data from the Denton County (in the Core area) of the Barnett shale, we found that 15% of the vertical and horizontal wells produce with a load recovery factor (LRF) of greater than unity. This implies 15% of these wells produce water from an 'external' source. This statistic might not be generalizable to the whole of the Barnett Shale. For the Parker County, we found that 15% of the horizontal wells produce water with a LRF greater than unity while 35% of the vertical wells produce water with a LRF greater than unity. A reasonable explanation of the results from Parker County is that the horizontal well fractures in Parker County tend to be contained despite the absence of a fracture barrier.

A neural network was developed to predict average water production for wells in both the Denton and Parker Counties. With rank in the input vector, the neural network

predicted average water production to within 10-26%. Also, we note that poor results are obtained if 'rank' is not used as a key parameter in the neural network input vector.

5.2 Recommendations

We note that petroleum engineering is a model and data intensive discipline. The models we use describe the system, whereas the system speaks, albeit in a metaphorical sense through data. We have in this work, focused on the use of data to extract information from shale gas reservoirs primarily because of the absence of numerical models that take the following into account; (1) the presence of an 'external' water source in the Barnett Shale, (2) capillary end effects peculiar to shale gas reservoirs and, (3) static and dynamic liquid loading. However, if such a model is developed, the data gained from model runs can be used to initialize a neural network. Actual production can thereafter be used to modify the network weights.

The dataset used in this study contained completion and production data. Important reservoir information that could provide the variability required in the dataset were not available. Hence, the development of a database with completion, production and reservoir variables would go a long way in reducing the mean error associated with the productivity predictions using virtual intelligence techniques.

REFERENCES

- Al-Fattah, S.M. and Startzman, R.A. 2003. Neural Network Approach Predicts U.S. Natural Gas Production. *SPEPF* **18**(2): 84-91. SPE-82411-PA.
- Al-Kaabi, A.U. and Lee, J.W. 1993. Using Artificial Neural Nets to Identify the Well-Test Interpretation Model. *SPEFE* **8**(3): 233-240. SPE 20332-PA.
- Aminian, K., Bilgesu, H.I., Ameri, S. and Gil, E. 2000. Improving the Simulation of Waterflood Performance with the use of Neural Networks. Paper SPE 65630 presented at the SPE Eastern Regional Meeting, Morgantown, West Virginia, USA., 17-19 October.
- Aminian, K., Ameri, S. and Bilgesu, H.I. 2002. A New Approach for Reservoir Characterization. Paper SPE 78710 presented at the SPE Eastern Regional Meeting, Lexington, Kentucky, USA., 23-25 October.
- Aminian, K., Ameri, S., Oyerokun, A. and Thomas, B. 2003a. Prediction of Flow Units and Permeability using Artificial Neural Networks. Paper SPE 83586 presented at the SPE Western Regional/American Association of Petroleum Geologists Pacific Section Joint Meeting, Long Beach, California, USA, 19-24 May.
- Aminian, K., Ameri, S., Bilgesu, H.I., Alla, V. and Mustafa, R. 2003b. Characterization of a Heterogeneous Reservoir in West Virginia. Paper SPE 84830 presented at the SPE Eastern Regional/American Association of Petroleum Geologists Eastern Section Joint Meeting, Pittsburgh, Pennsylvania, USA, 6-10 September.
- Arpat, B.G., Caers, J. and Haas, A. 2001. Characterization of West-Africa Submarine Channel Reservoirs: A Neural Network Based Approach to Integration of Seismic

- Data. Paper SPE 71345 presented at the SPE Annual Technical Conference and Exhibition, New Orleans, Louisiana, USA, 30 September-3 October.
- Artun, E., Ertekin, T., Watson, R. and Miller, B. 2008. Optimized Design of Cyclic Pressure Pulsing in a Depleted Naturally Fractured Reservoir. Paper SPE 117762 presented at the SPE Eastern Regional/American Association of Petroleum Geologists Eastern Section Joint Meeting, Pittsburgh, Pennsylvania, USA, 11-15 October.
- Athichanagorn, S. and Horne, R.N. 1995. Automatic Parameter Estimation From Well Test Data Using Artificial Neural Network. Paper SPE 30556 presented at the SPE Annual Technical Conference and Exhibition, Dallas, Texas, USA, 22-25 October.
- Ayala, L.F. and Ertekin, T. 2005. Analysis of Gas-Cycling Performance in Gas/Condensate Reservoirs using Neuro-Simulation. Paper SPE 95655 presented at the SPE Annual Technical Conference and Exhibition, Dallas, Texas, USA, 9-12 October.
- Ayala, L.F. and Ertekin, T. 2007. Study of Gas/Condensate Reservoir Exploitation Using Neuro-Simulation. *SPEE* **10**(2): 140-149. SPE-88471-PA.
- Balch, R.S., Stubbs, B.S., Weiss, W.W. and Wo, S. 1999. Using Artificial Intelligence to Correlate Multiple Seismic Attributes to Reservoir Properties. Paper SPE 56733 presented at the SPE Annual Technical Conference and Exhibition, Houston, Texas, USA, 3-6 October.
- Balch, R.S., Hart, D.M., Weiss, W.W. and Broadhead, R.F. 2002. Regional Data Analysis to Better Predict Drilling Success: Brushy Canyon Formation, Delaware Basin, New Mexico. Paper SPE 75145 presented at the SPE/DOE Improved Oil Recovery Symposium, Tulsa, Oklahoma, USA, 13-17 April.

- Basbug, B. and Karpyn, Z. 2007. Estimation of Permeability from Porosity, Specific Surface Area, and Irreducible Water Saturation Using an Artificial Neural Network. Paper SPE 107909 presented at the SPE Latin American and Caribbean Petroleum Engineering Conference, Buenos Aires, Argentina, 15-18 April.
- Bilgesu, H.I., Tetrick, L.T., Altmis, U., Mohaghegh, S. and Ameri, S. 1997. A New Approach for the Prediction of Rate of Penetration (ROP) Values. Paper SPE 39231 presented at the SPE Eastern Regional Meeting, Lexington, Kentucky, USA, 22-24 October.
- Bilgesu, H.I., Al-Rashidi, A.F., Aminian, K. and Ameri, S. 2000. A New Approach for Drill Bit Selection. Paper SPE 65618 presented at the SPE Eastern Regional Meeting, Morgantown, West Virginia, USA, 17-19 October.
- Caers, J. and Journel, A.G. 1998. Stochastic Reservoir Simulation using Neural Networks Trained on Outcrop Data. Paper SPE 49026 presented at the SPE Annual Technical Conference and Exhibition, New Orleans, Louisiana, USA, 27-30 September.
- Caers, J., Srinivasan, S. and Journel, A.G. 1999. Geostatistical Quantification of Geological Information for a Fluvial-type North Sea Reservoir. Paper SPE 56655 presented at the SPE Annual Technical Conference and Exhibition, Houston, Texas, USA, 3-6 October.
- Centilmen, A., Ertekin, T. and Grader, A.S. 1999. Applications of Neural Networks in Multi-Well Field Development. Paper SPE 56433 presented at the SPE Annual Technical Conference and Exhibition, Houston, Texas, USA, 3-6 October.
- Chan, K.S. 1995. Water Control Diagnostic Plots. Paper SPE 30775 presented at the SPE Annual Technical Conference and Exhibition, Dallas, Texas, USA, 22-25 October.

- Chang, S., Grigg, R.B. and Sung, A.H. 2000. Use of MASTER Web to Improve History Matching. Paper SPE 62617 presented at the SPE/American Association of Petroleum Geologists Western Regional Meeting, Long Beach, California, USA, 19-23 June.
- Chawanthe, A.1994. The Application of Kohonen Type Self Organization Algorithm to Formation Evaluation. Paper 29179 presented at the SPE Eastern Regional Conference and Exhibition, Charleston, West Virginia, U.S.A., 8-10 November.
- Chawanthe, A. and Ye, M. 1997. Neural Vector Quantization for Multivariate Upscaling. Paper SPE 37989 presented at the SPE Reservoir Simulation Symposium, Dallas, Texas, USA, 8-11 June.
- Cybenko, G. 1989. Approximations by superposition of a sigmoidal function. *Mathematics of Control, Signals, and Systems*, **2**: 303-314.
- Demiryurek, U., Banaei-Kashani, F. and Shahabi, C., 2008. Neural-Network Based Sensitivity Analysis for Injector-Producer Relationship Identification. Paper SPE 112124 presented at the SPE Intelligent Energy Conference and Exhibition, Amsterdam, The Netherlands, 25-27 February.
- Doraisamy, H. 1998a. Methods of Neuro-Simulation for Field Development. Paper SPE 39962 presented at the Rocky Mountain/Low Permeability Reservoir Regional Meeting, Denver, Colorado, USA, 5-8 April.
- Doraisamy, H., Ertekin, T. and Grader, A.S. 1998b. Key Parameters Controlling the Performance of Neuro-simulation Applications in Field Development. Paper SPE 51079 presented at the SPE Eastern Regional Meeting, Pittsburgh, Pennsylvania, USA, 9 – 11 November.

- Friedel, T., Mtchedlishvili, G., Behr, A., Voigt, H. and Frieder, H. 2007. Comparative Analysis of Damage Mechanisms in Fractured Gas Wells. Paper SPE 107662 presented at the SPE European Formation Damage Conference, Scheveningen, The Netherlands, 30 May – 1 June.
- Garcia, A. and Mohaghegh, S. 2004. Forecasting U.S. Natural Gas Production into year 2020: A Comparative Study. Paper SPE 91413 presented at the SPE Eastern Regional Conference and Exhibition, Charleston, West Virginia, USA, 15-17 September.
- Garg, A., Kovscek, A.R., Nikraves, M., Castanier, L.M. and Patzek, T.W. 1996. CT Scan and Neural Network Technology for Construction of Detailed Distribution of Residual Oil Saturation During Water-flooding. Paper SPE 35737 presented at the Western Regional Meeting, Anchorage, Alaska, USA, 22-24 May.
- Gorucu, F. B., Ertekin, T., Bromhal, G.S., Smith, D.H., Sams, W.N. and Jikich, S.A. 2005. A Neurosimulation Tool for Predicting Performance in Enhanced Coalbed Methane and CO₂ Sequestration Projects. Paper SPE 97164 presented at the SPE Annual Technical Conference and Exhibition, Dallas, Texas, USA, 9-12 October.
- Guyaguler, B., Horne, R.N., Rogers, L. and Rosenzweig, J.J. 2000. Optimization of Well Placement in a Gulf of Mexico Waterflooding Project. Paper SPE 63221 presented at the SPE Annual Technical Conference and Exhibition, Dallas, Texas, USA, 1-4 October.
- Habiballah, W.A., Startzman, R.A. and Barrufet, M.A. 1996. Use of Neural Networks for Prediction of Vapor/Liquid Equilibrium K Values for Light – Hydrocarbon Mixtures. *SPEE* 11(2): 121-126. SPE-28597-PA.

- Haykin, S. 2005. *Neural Networks, a Comprehensive Foundation*. Ninth Indian Reprint. Dehli, India: Pearson Prentice Hall.
- Holditch, S.A. 1979. Factors Affecting Water Blocking and Gas Flow from Hydraulically Fractured Wells. *JPT* **31**(12): 1515-1524. SPE-7561-PA.
- Hornik, K., Stinchcombe, M. and White, H. 1989. Multilayer feedforward neural networks are universal approximators. *Neural Networks*, **2**: 359-366.
- Hosn, N.A., Popa, A.S. and Popa, C.G. 2001. A New and Realistic Approach to Pumping Unit Optimization through the Use of Intelligent Systems. Paper SPE 72360 presented at the SPE Eastern Regional Meeting, Canton, Ohio, USA, 17-19 October.
- Iqbal, G.M.M. 1988. Cleanup of water based liquids from hydraulically fractured gas wells. PhD dissertation, The University of Oklahoma, Norman, Oklahoma.
- Kaviani, D., Bui, T.D., Jensen, J.L. and Hanks, C.L. 2008. The Application of Artificial Neural Networks with Small Data Sets: An Example for Analysis of Fracture Spacing in the Lisburne Formation, Northeastern Alaska. *SPEEE* **11**(3): 598-605. SPE-103188-PA.
- Kumoluyi, A.O. and Daltaban, T.S. 1994. Higher Order Neural Networks in Petroleum Engineering. Paper SPE 27905 presented at the SPE Western Regional Meeting, Long Beach, California, USA, 23-25 March.
- Kumoluyi, A.O. and Daltaban, T.S., Archer, J.S. 1995. Identification of Well-Test Models by Use of Higher Order Neural Networks. *SPECA* **4**(2): 146-150. SPE-27558-PA.

- Lee, S.H., Kharghoria, A. and Datta-Gupta, A. 2002. Electrofacies Characterization and Permeability Predictions in Complex Reservoirs. *SPEEE* 5(3): 237-248. SPE-78662-PA.
- Martineau, D.F. 2007. History of the Newark East Field and the Barnett shale as a gas reservoir. *AAPG Bulletin* 91(4): 399-403.
- Mitchell, T. 1997. Machine Learning. International Edition. Singapore: McGraw-Hill Book Co.
- Mohaghegh, S., Balan, B. and Ameri, S. 1995a. State-of-The-Art in Permeability Determination from Well Log Data: Part2- Verifiable, Accurate Permeability Predictions, the Touch-Stone of All Models. Paper SPE 30979 presented at the SPE Eastern Regional Conference and Exhibition, Morgantown, West Virginia, USA, 18-20 September.
- Mohaghegh, S., Arefi, R., Bilgesu, I., Ameri, S. and Rose, D. 1995b. Design and Development of an Artificial Neural Network for Estimation of Formation Permeability. *SPECA* 1(3): 151-154. SPE-28237-PA.
- Mohaghegh, S., Balan, B., Ameri, S. and McVey, D.S. 1996a. A Hybrid, Neuro-Genetic Approach to Hydraulic Fracture Treatment Design and Optimization. Paper SPE 36602 presented at the SPE Annual Technical Conference and Exhibition, Denver, Colorado, USA, 6-9 October.
- Mohaghegh, S., Hefner, H.M. and Ameri, S. 1996b. Fracture Optimization eXpert (FOX) – How Computational Intelligence Helps the Bottom-Line in Gas Storage. Paper SPE 37341 presented at the SPE Eastern Regional Conference, Columbus, Ohio, USA, 23-25 October.

- Mohaghegh, S., Balan, B., Ameri, S. and McVey, D.S. 1997. Permeability Determination from Well Log Data. *SPEFE* **12**(3): 170-174. SPE-30978-PA.
- Mohaghegh, S., Richardson, M. and Ameri, S. 1998a. Virtual Magnetic Imaging Logs: Generation of Synthetic MRI Logs from Conventional Well Logs. Paper SPE 51075 presented at the SPE Eastern Regional Meeting, Pittsburgh, PA, USA, 9-11 November.
- Mohaghegh, S., Platon, V. and Ameri, S. 1998b. Candidate Selection for Stimulation of Gas Storage Wells Using Available Data with Neural Networks and Genetic Algorithms. Paper SPE 51080 presented at the SPE Eastern Regional Meeting, Pittsburgh, PA, USA, 9-11 November.
- Mohaghegh, S., Mohamad, K., Popa, A. and Ameri, S. 1999. Performance Drivers in Restimulation of Gas Storage Wells. Paper SPE 57453 presented at the SPE Eastern Regional Meeting, Charleston, West Virginia, USA, 21-22 October.
- Mohaghegh, S. 2000a. Permeability Virtual-Intelligence Applications in Petroleum Engineering: Part 1 – Artificial Neural Networks. *JPT* **52**(9): 64-73. SPE-58046.
- Mohaghegh, S. 2000b. Permeability Virtual-Intelligence Applications in Petroleum Engineering: Part 2 – Evolutionary Computing. *JPT* **52**(10): 40-46. SPE-61925.
- Mohaghegh, S. 2000c. Permeability Virtual-Intelligence Applications in Petroleum Engineering: Part 3 – Fuzzy Logic. *JPT* **52**(11): 82-87. SPE-62415.
- Mohaghegh, S., Reeves, S. and Hill, D. 2000d. Development of an Intelligent Systems Approach for Restimulation Candidate Selection. Paper SPE 59767 presented at the SPE/CERI Gas Technology Symposium, Calgary, Alberta, Canada, 3-5 April.

- Mohaghegh, S., Goodard, C., Popa, A., Ameri, S. and Bhuiyan, M. 2000e. Reservoir Characterization Through Synthetic Logs. Paper SPE 65675 presented at the SPE Eastern Regional Meeting, Morgantown, West Virginia, USA, 17-19 October.
- Mohaghegh, S., Hutchins, L.A. and Sisk, C.D. 2002. Prudhoe Bay Oil Production Optimization: Using Virtual Intelligence Techniques, Stage One: Neural Model Building. Paper SPE 77659 presented at the SPE Annual Technical Conference and Exhibition, San Antonio, Texas, USA, 29 September – 2 October.
- Mohaghegh, S. 2003. Essential Components of an Integrated Data Mining Tool for the Oil and Gas Industry, With an Example in the DJ Basin. Paper SPE 84441 presented at the SPE Annual Technical Conference and Exhibition, Denver, Colorado, USA, 5-8 October.
- Mohaghegh, S., Modavi, A., Hafez, M., Haajizadeh, M., Kenawy, M. and Guruswamy, S. 2006a. Development of Surrogate Reservoir Models (SRM) for Fast-Track Analysis of Complex Reservoirs. Paper SPE 99667 presented at the SPE Intelligent Energy Conference and Exhibition, Amsterdam, The Netherlands, 11-13 April.
- Mohaghegh, S. 2006b. Quantifying Uncertainties Associated with Reservoir Simulation Studies Using Surrogate Reservoir Models. Paper SPE 102492 presented at the SPE Annual Technical Conference and Exhibition, San Antonio, Texas, USA, 24-27 September.
- Montgomery, K.T., Holditch, S.A. and Berthelot, J.M. 1990. Effects of Fracture Fluid Invasion on Cleanup Behavior and Pressure Buildup Analysis. Paper SPE 20643 presented at the SPE Annual Technical Conference and Exhibition, New Orleans, LA, USA, 23-26 September.

- Montgomery, S.L., Jarvie, D. M., Bowler, K.A. and Pollastro, R.M. 2005. Missippian Barnett Shale, Fort Worth Basin, North-Central Texas: Gas-shale play with multi-trillion cubic foot potential. *AAPG Bulletin* **89**(2): 155-175.
- Ouenes, A., Bhagavan, S., Bunge, P.H. and Travis, B.J. 1994. Application of Simulated Annealing and Other Global Optimization Methods to Reservoir Description: Myths and Realities. Paper SPE 28415 presented at the SPE Annual Technical Conference and Exhibition, New Orleans, LA, USA, 25-28 September.
- Ouenes, A., Richardson, S. and Weiss, W.W. 1995. Fractured Reservoir Characterization and Performance Forecasting Using Geomechanics and Artificial Intelligence. Paper SPE 30572 presented at the SPE Annual Technical Conference and Exhibition, Dallas, TX, USA, 22-25 October.
- Pollastro, R.M., Jarvie, D. M., Hill, R.J. and Adams, C.W. 2007. Geologic framework of the Missippian Barnett Shale, Barnett-Paleozoic total petroleum system, Bend Arch-Fort Worth Basin, Texas. *AAPG Bulletin* **91**(4): 405-436.
- Popa, A.S., Mohaghegh, S.D., Gaskari, R. and Ameri, S. 2003. Identification of Contaminated Data in Hydraulic Fracturing Databases: Application to the Codell Formation in the DJ Basin. Paper SPE 83446 presented at the SPE Western Regional/American Association of Petroleum Geologists Pacific Section Joint Meeting, Long Beach, CA, USA, 19-24 May.
- Popa, A., Ramos, R., Cover, A. and Popa, C. 2005. Integration of Artificial Intelligence and Lean Sigma for Large-Field Production Optimization: Application to Kern River Field. Paper SPE 97247 presented at the SPE Annual Technical Conference and Exhibition, Dallas, TX, USA, 9-12 October.

- Ramgulam, A., Ertekin, T. and Flemings, P.B. 2007. Utilization of Artificial Neural Networks in the Optimization of History Matching. Paper SPE 107468 presented at the SPE Latin American and Caribbean Petroleum Engineering Conference, Buenos Aires, Argentina, 15-18 April.
- Reeves, S.R., Hill, D.G., Tiner, R.L., Bastian, P.A., Conway, M.W. and Mohaghegh, S. 1999a. Restimulation of Tight Gas Sand Wells in the Rocky Mountain Region. Paper SPE 55627 presented at the SPE Rocky Mountain Regional Meeting, Gillette, Wyoming, USA, 15-18 May.
- Reeves, S.R., Hill, D.G., Tiner, R.L., Hopkins, C.W., Conway, M.W. and Mohaghegh, S. 1999b. Restimulation Technology for Tight Gas Sand Wells. Paper SPE 56482 presented at the SPE Annual Technical Conference and Exhibition, Houston, TX, USA, 3-6 October.
- Saeedi, A., Camarda, K.V. and Liang, J.T. 2007. Using Neural Networks for Candidate Selection and Well Performance Prediction in Water-Shutoff Treatments Using Polymer Gels – A Field-Case Study. *SPEPO* **22**(4): 417-424. SPE-101028-PA.
- Seright, R.S. 1997. Improved Methods for Water Shutoff. Annual Report, Contract No. DE-AC22-94PC91008, Subcontract No. G4S60330, US DOE, Oklahoma (November 1997).
- Shelley B., Johnson, B.J., Fielder, E.O., Heinze, J.R. and Werline, J.R. 2008. Data Analysis of Barnett Shale Completions. *SPEJ* **13**(3): 366-374. SPE-100674-PA.
- Shelley B. and Harris, P.C. 2009. Data Mining Identifies Production Drivers in a Complex High-Temperature Gas Reservoir. *SPEPO* **24**(1): 74-80. SPE-106463-PA.

- Shippen, M.E. and Scott, S.L. 2004. A Neural Network Model for Prediction of Liquid Holdup in Two-Phase Horizontal Flow. *SPEPF* **19**(2): 67-76. SPE-87682-PA.
- Silpngarmlers, N. and Ertekin, T. 2002. Artificial Neural Network Architectures for Predicting Two-Phase and Three-Phase Relative Permeability Characteristics. Paper SPE 77704 presented at the SPE Annual Technical Conference and Exhibition, San Antonio, TX, USA, 29 September - 2 October.
- Soliman, M.Y. and Hunt, J.L. 1985. Effect of Fracturing Fluid and Its Cleanup on Well Performance. Paper SPE 14514 presented at the SPE Eastern Regional Meeting, Morgantown, West Virginia, USA, 6 – 8 November.
- Solomon, F.A., Falcone, G. and Teodoriu, C. 2008. Critical Review of Existing Solutions to Predict and Model Liquid Loading in Gas Wells. Paper SPE 115933 presented at the SPE Annual Technical Conference and Exhibition, Denver, Colorado, USA, 21-24 September.
- Srinivasan, S. and Caers, J. 2000. Conditioning Reservoir Models to Dynamic Data – A Forward Modeling Perspective. Paper SPE 62941 presented at the SPE Annual Technical Conference and Exhibition, Dallas, TX, USA, 1 - 4 October.
- Srinivasan, S. and Ertekin, T. 2008. Development and Testing of an Expert System for Coalbed Methane Reservoirs Using Artificial Neural Networks. Paper SPE 119935 presented at the SPE Eastern Regional/American Association of Petroleum Geologists Eastern Section Joint Meeting, Pittsburgh, PA, USA, 11 - 15 October.
- Tannich, J.D. 1975. Liquid removal from hydraulically fractured gas wells. *JPT* **27**(11): 1309-1317. SPE-5113-PA.

- Turner, R.G., Hubbard, J.D. and Dukler, A.E. 1969. Analysis and prediction of minimum flow rate for the continuous removal of liquids from gas wells. *JPT* **21**(11): 1475-1482. SPE-2198-PA.
- Wei, M., Sung, A.H. and Cather, M., 2004. A Methodology to Discover Contaminated Data in Spatial Databases. Paper SPE 90267 presented at the SPE Annual Technical Conference and Exhibition, Houston, TX, USA, 26-29 September.
- Wo, S., Weiss, W.W., Balch, R.S., Scott, L.R. and Kendall, R.P. 2000. A New Technique to Determine Porosity and Deep Resistivity from Old Gamma Ray and Neutron Count Logs. Paper SPE 59553 presented at the SPE Permian Basin Oil and Gas Recovery Conference, Midland, TX, USA, 21-23 March.
- Yeten, B., Durlofsky, L.J. and Aziz, K. 2002. Optimization of Non-Conventional Well Type, Location and Trajectory. Paper SPE 77565 presented at the SPE Annual Technical Conference and Exhibition, San Antonio, TX, USA, 29 September-2 October.
- Zellou, A.M., Ouenes, A. and Banik, A.K. 1995. Improved Fractured Reservoir Characterization Using Neural Networks, Geomechanics and 3-D Seismic. Paper SPE 30722 presented at the SPE Annual Technical Conference and Exhibition, Dallas, TX, USA, 22-25 October.

APPENDIX A

TABLE A-1 – STATISTICAL ANALYSIS OF DATA FROM DENTON COUNTY									
	<u>Gas (Mcf/mth)</u>			<u>Water (bbls/mth)</u>			<u>WHP (psi)</u>		
	<u>P10</u>	<u>P50</u>	<u>P90</u>	<u>P10</u>	<u>P50</u>	<u>P90</u>	<u>P10</u>	<u>P50</u>	<u>P90</u>
Deviated	3535	6427	11898	0	99	293	50	200	356
Horizontal	7053	20716	39689	0	229	1540	0	180	328
Vertical	2244	5184	10430	45	132	566	90	220	405

TABLE A-2 – STATISTICAL ANALYSIS OF DATA FROM TARRANT COUNTY									
	<u>Gas (Mcf/mth)</u>			<u>Water (bbls/mth)</u>			<u>WHP (psi)</u>		
	<u>P10</u>	<u>P50</u>	<u>P90</u>	<u>P10</u>	<u>P50</u>	<u>P90</u>	<u>P10</u>	<u>P50</u>	<u>P90</u>
Deviated	2827	8267	16841	29	102	565	0	263	366
Horizontal	9789	29996	62205	0	95	2574	0	0	300
Vertical	1912	7792	15485	29	127	527	0	250	420

TABLE A-3 – STATISTICAL ANALYSIS OF DATA FROM WISE COUNTY									
	<u>Gas (Mcf/mth)</u>			<u>Water (bbls/mth)</u>			<u>WHP (psi)</u>		
	<u>P10</u>	<u>P50</u>	<u>P90</u>	<u>P10</u>	<u>P50</u>	<u>P90</u>	<u>P10</u>	<u>P50</u>	<u>P90</u>
Deviated	4393	8815	15062	0	66	270	130	190	304
Horizontal	6107	22703	41445	0	148	1481	0	112	296
Vertical	2017	6431	13188	0	109	567	55	185	310

TABLE A-4 – STATISTICAL ANALYSIS OF DATA FROM ERATH COUNTY

	<u>Gas (Mcf/mth)</u>			<u>Water (bbls/mth)</u>			<u>WHP (psi)</u>		
	<u>P10</u>	<u>P50</u>	<u>P90</u>	<u>P10</u>	<u>P50</u>	<u>P90</u>	<u>P10</u>	<u>P50</u>	<u>P90</u>
Horizontal	1980	6793	14593	0	0	1642	0	0	126
Vertical	291	646	6906	0	57	1723	0	40	188

TABLE A-5 – STATISTICAL ANALYSIS OF DATA FROM HOOD COUNTY

	<u>Gas (Mcf/mth)</u>			<u>Water (bbls/mth)</u>			<u>WHP (psi)</u>		
	<u>P10</u>	<u>P50</u>	<u>P90</u>	<u>P10</u>	<u>P50</u>	<u>P90</u>	<u>P10</u>	<u>P50</u>	<u>P90</u>
Horizontal	4841	13134	24669	0	0	3548	0	0	320
Vertical	247	432	3650	0	981	2862	0	0	62

TABLE A-6 – STATISTICAL ANALYSIS OF DATA FROM JACK COUNTY

	<u>Gas (Mcf/mth)</u>			<u>Water (bbls/mth)</u>			<u>WHP (psi)</u>		
	<u>P10</u>	<u>P50</u>	<u>P90</u>	<u>P10</u>	<u>P50</u>	<u>P90</u>	<u>P10</u>	<u>P50</u>	<u>P90</u>
Horizontal	3093	8331	14977	0	338	7105	0	54	176
Vertical	213	1799	4265	0	158	1966	0	55	201

TABLE A-7 – STATISTICAL ANALYSIS OF DATA FROM JOHNSON COUNTY

	<u>Gas (Mcf/mth)</u>			<u>Water (bbls/mth)</u>			<u>WHP (psi)</u>		
	<u>P10</u>	<u>P50</u>	<u>P90</u>	<u>P10</u>	<u>P50</u>	<u>P90</u>	<u>P10</u>	<u>P50</u>	<u>P90</u>
Horizontal	9208	25155	54852	0	258	3621	93	136	256
Vertical	770	4724	38152	0	161	3568	0	103	314

TABLE A-8 – STATISTICAL ANALYSIS OF DATA FROM PALO PINTO COUNTY

	<u>Gas (Mcf/mth)</u>			<u>Water (bbls/mth)</u>			<u>WHP (psi)</u>		
	<u>P10</u>	<u>P50</u>	<u>P90</u>	<u>P10</u>	<u>P50</u>	<u>P90</u>	<u>P10</u>	<u>P50</u>	<u>P90</u>
Horizontal	2082	9016	15227	0	0	4989	0	0	170.5
Vertical	380	1315	2065	0	93	2739	0	45	202

TABLE A-9 – STATISTICAL ANALYSIS OF DATA FROM PARKER COUNTY

	<u>Gas (Mcf/mth)</u>			<u>Water (bbls/mth)</u>			<u>WHP (psi)</u>		
	<u>P10</u>	<u>P50</u>	<u>P90</u>	<u>P10</u>	<u>P50</u>	<u>P90</u>	<u>P10</u>	<u>P50</u>	<u>P90</u>
Horizontal	2986	11926	27712	0	0	4312	0	103	300
Vertical	424	2295	5165	0	112	704	0	150	400

TABLE A-10– STATISTICAL ANALYSIS OF DATA FROM SOMERVELL COUNTY

	<u>Gas (Mcf/mth)</u>			<u>Water (bbls/mth)</u>			<u>WHP (psi)</u>		
	<u>P10</u>	<u>P50</u>	<u>P90</u>	<u>P10</u>	<u>P50</u>	<u>P90</u>	<u>P10</u>	<u>P50</u>	<u>P90</u>
Horizontal	2964	10011	25565	0	0	3395	0	93.5	183.8

VITA

Name: Obadare Olusegun Awoleke

Address: Department of Petroleum Engineering,
3116 TAMU, 507 Richardson Building,
College Station, TX-77843-3116.

Education: B.Sc. Petroleum Engineering, University of Ibadan, Nigeria, 2001.
M.S. Petroleum Engineering, Texas A&M University, 2009.

Work Experience: Engineer (Cement, Acid and Coil Tubing), BJ Services Nigeria
(2003-2007)